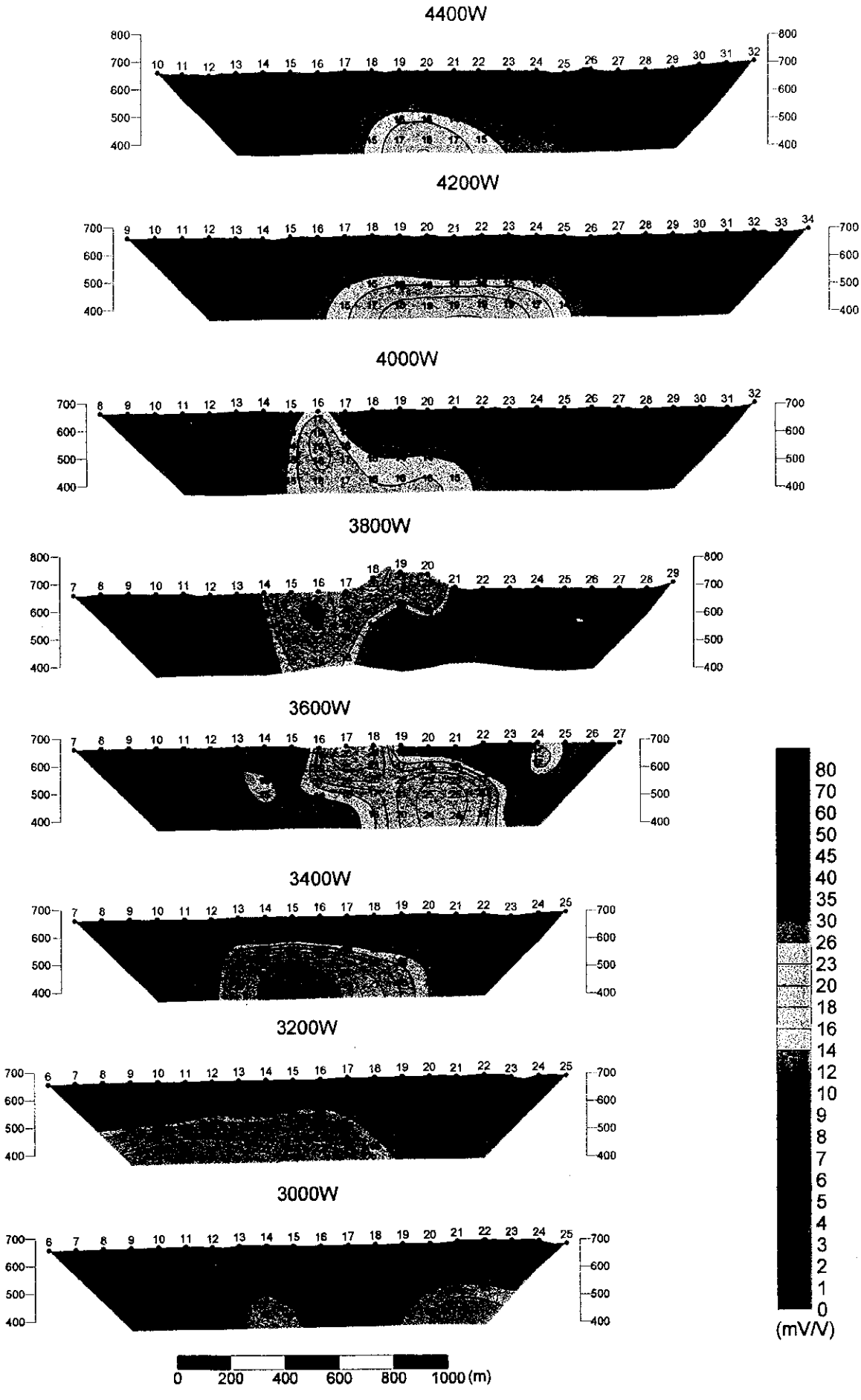

Fig. II -5-25(2) 2D analysis sections for chargeability in Hayl as Safil area

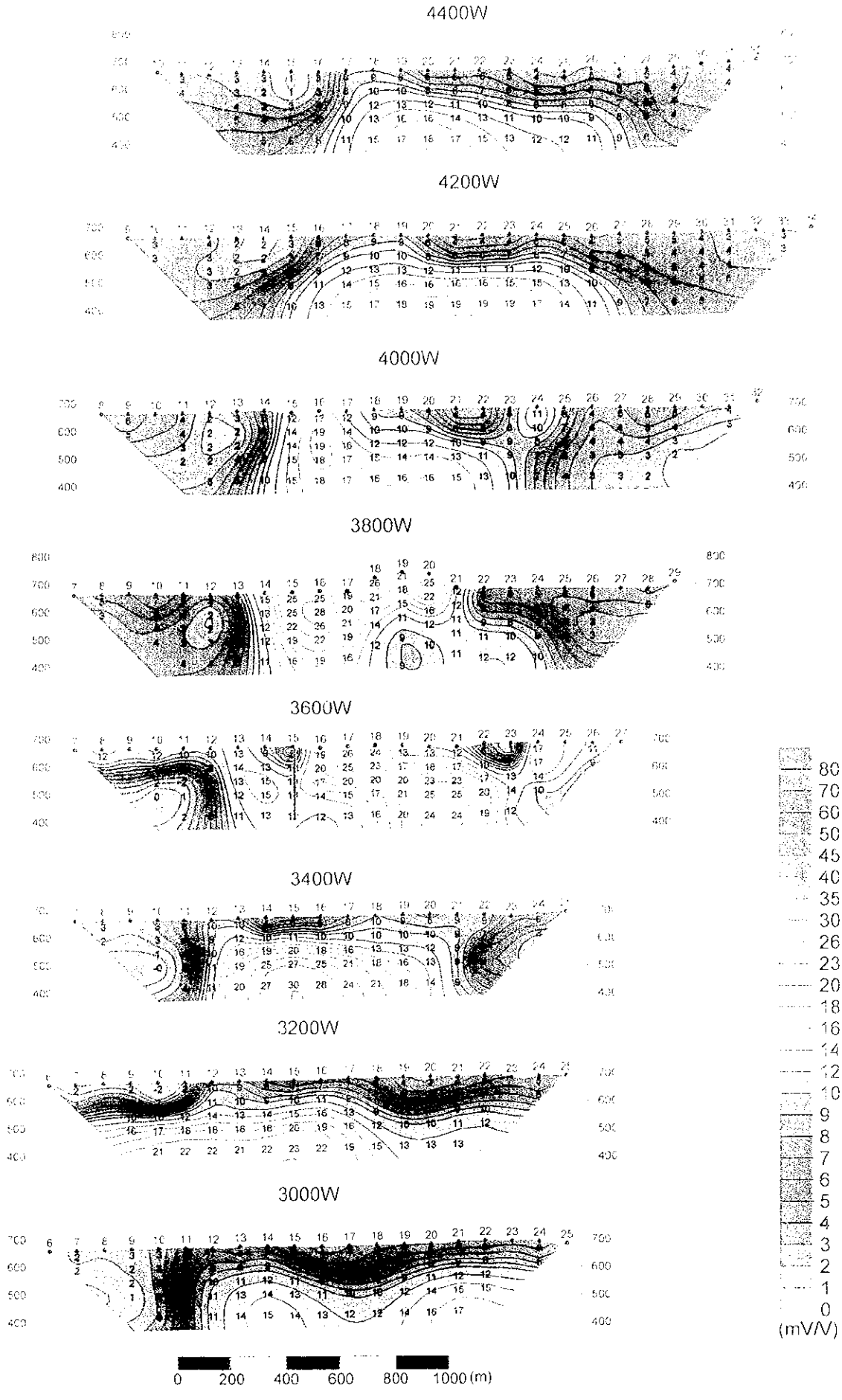

Fig. II -5-25(2) 2D analysis sections for chargeability in Hayl as Safil area

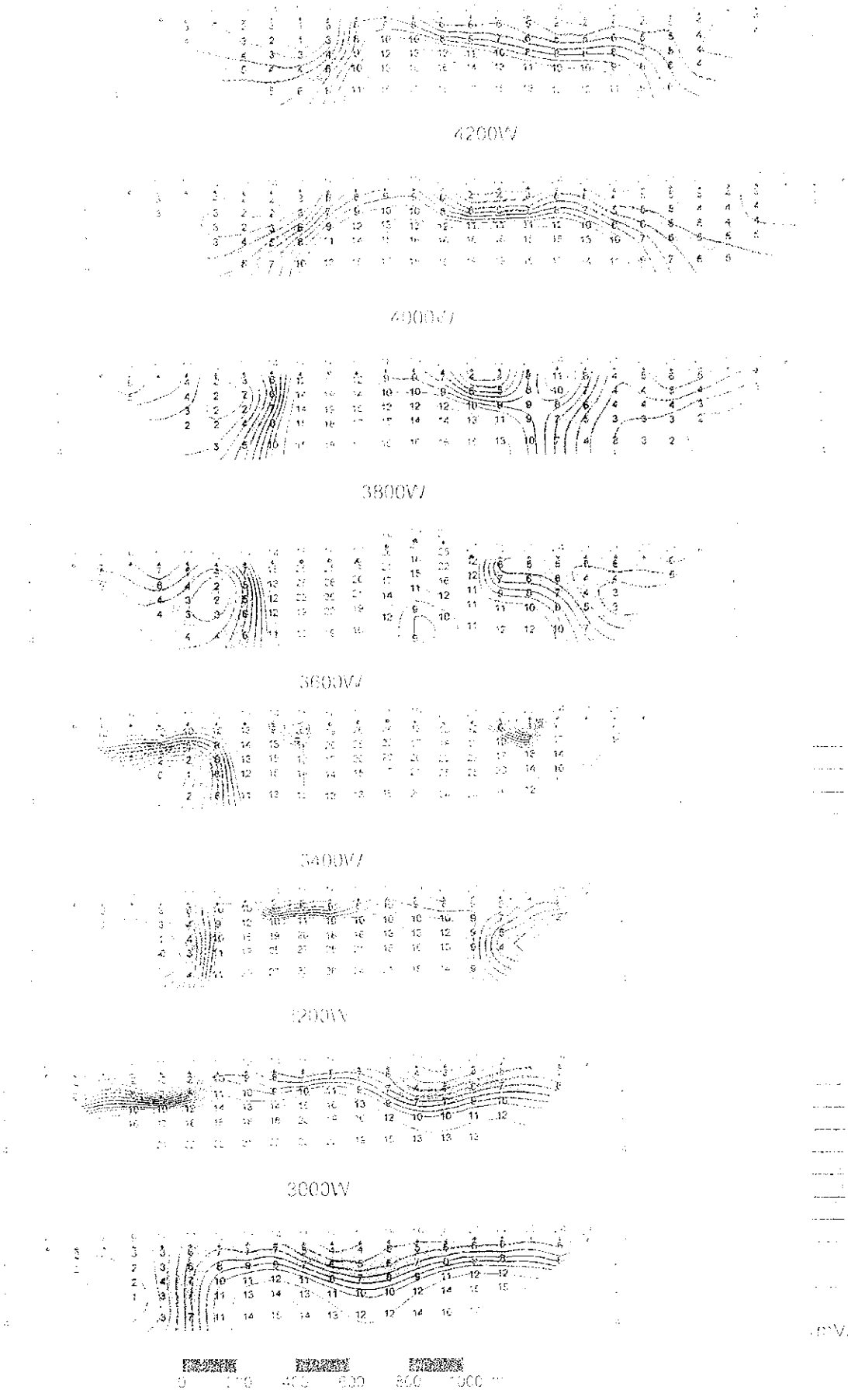

Fig. 1. 2D analysis sections for chargeability in Hayllas Salt Lake

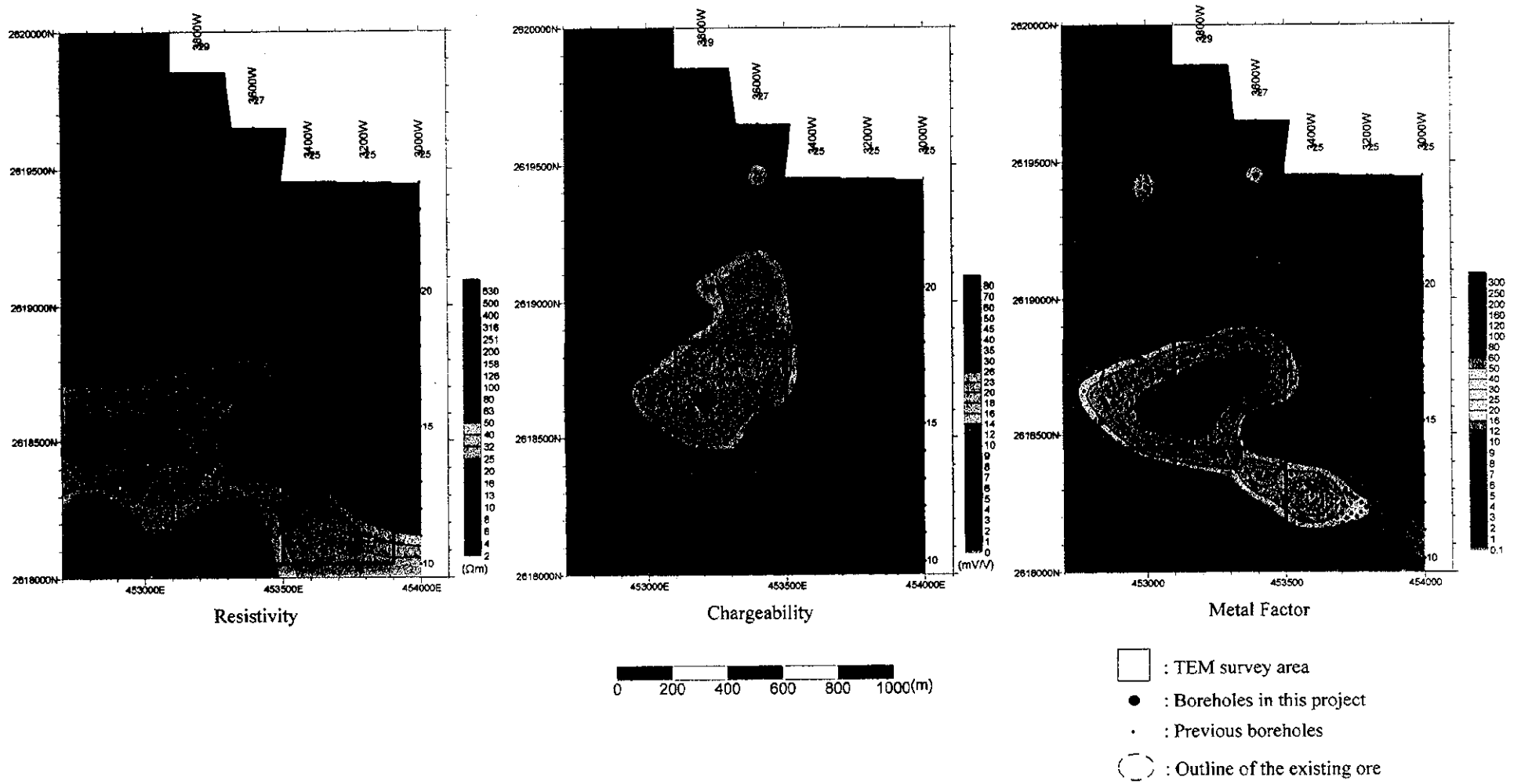

Fig. II -5-26(1) 2D analysis plane maps in Hayl as Safil area at 100m depth

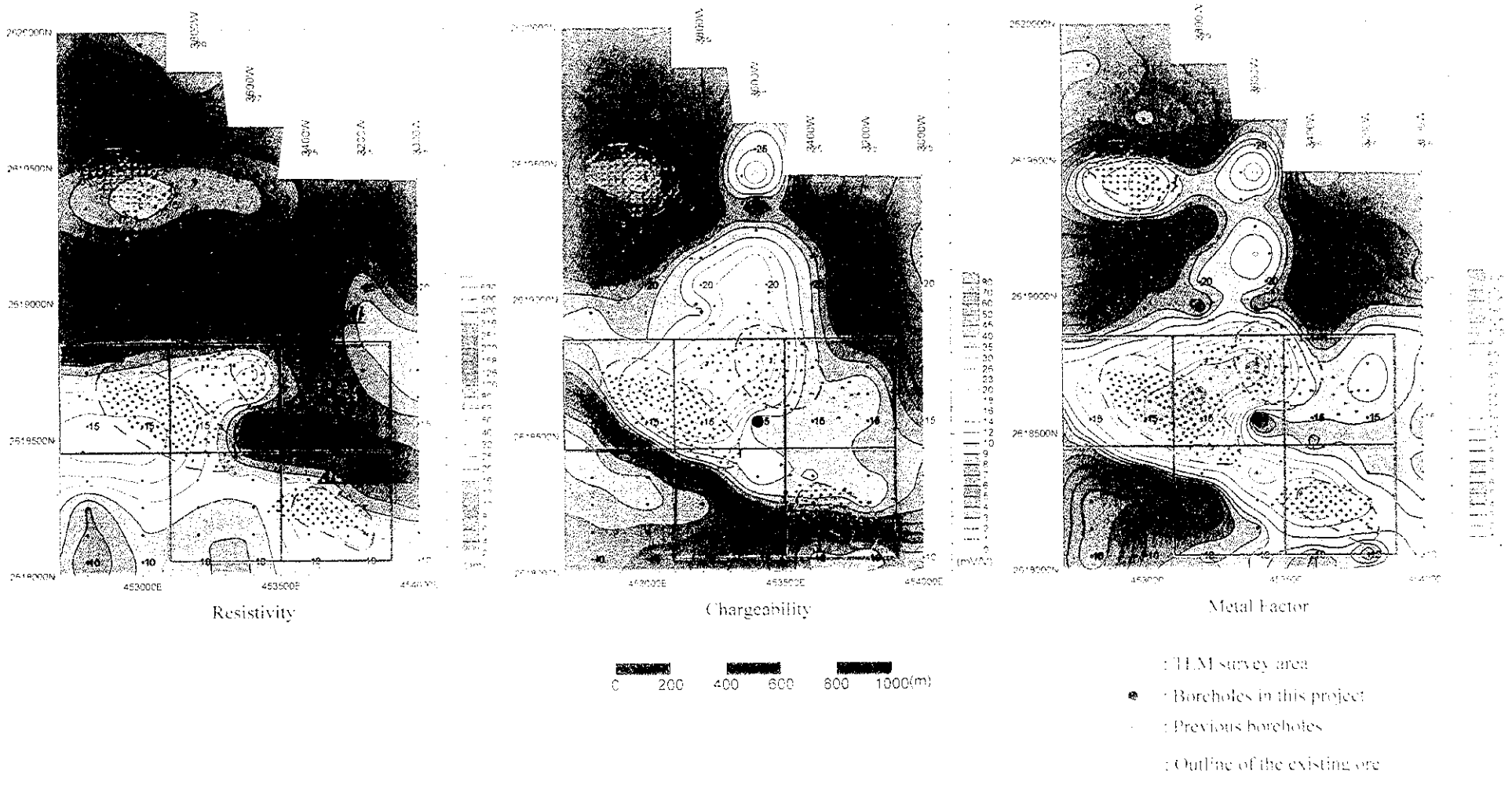

Fig. II-5-26(1) 2D analysis plane maps in Hayl as Safil area at 100m depth

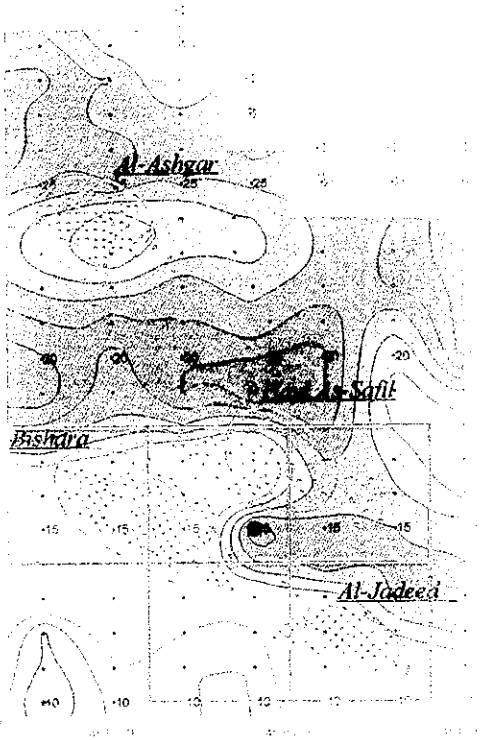
Al-Ashqar
Ras As-Safit
Bishdra
Al-Jadeed

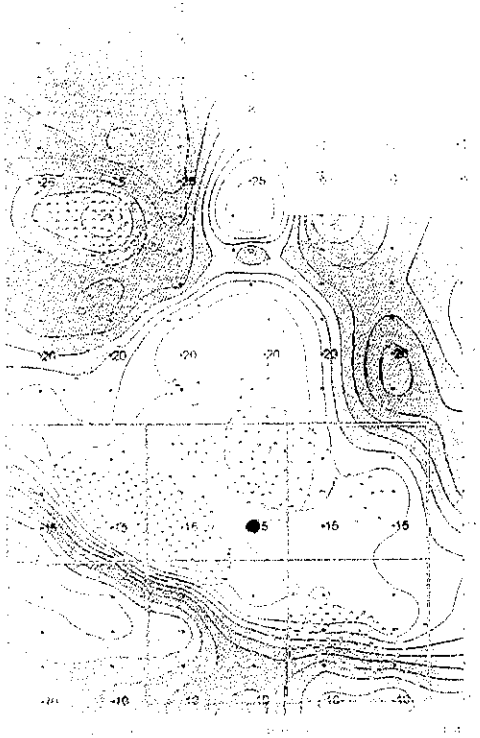

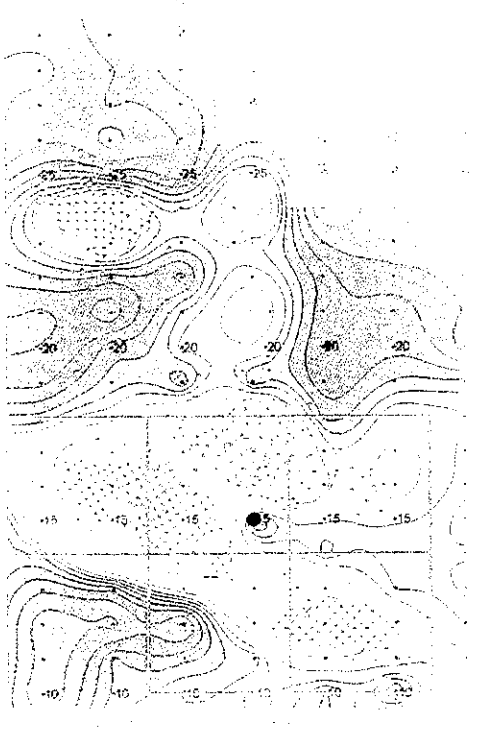

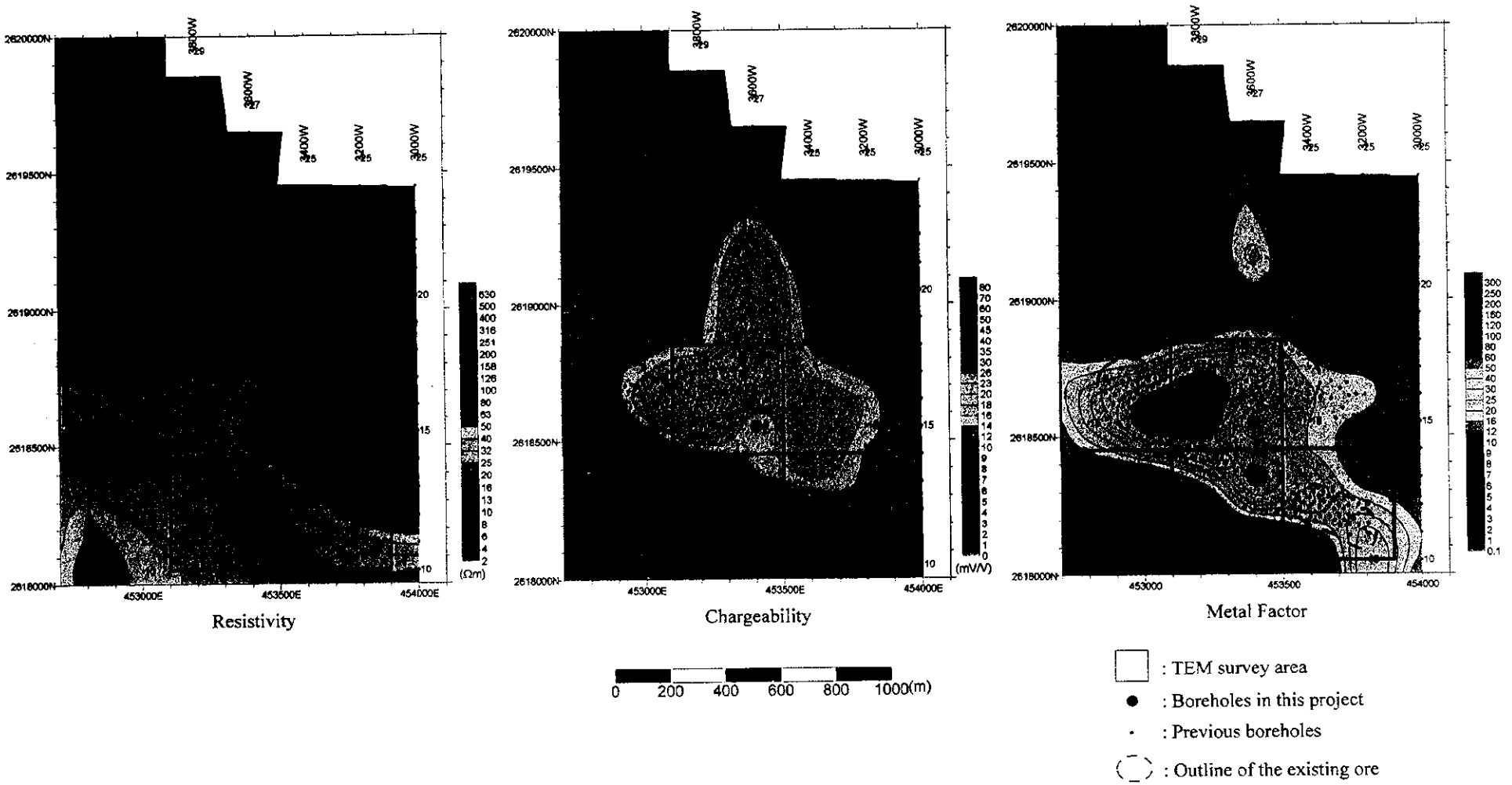

Fig. II-5-26(2) 2D analysis plane maps in Hayl as Safil area at 150m depth

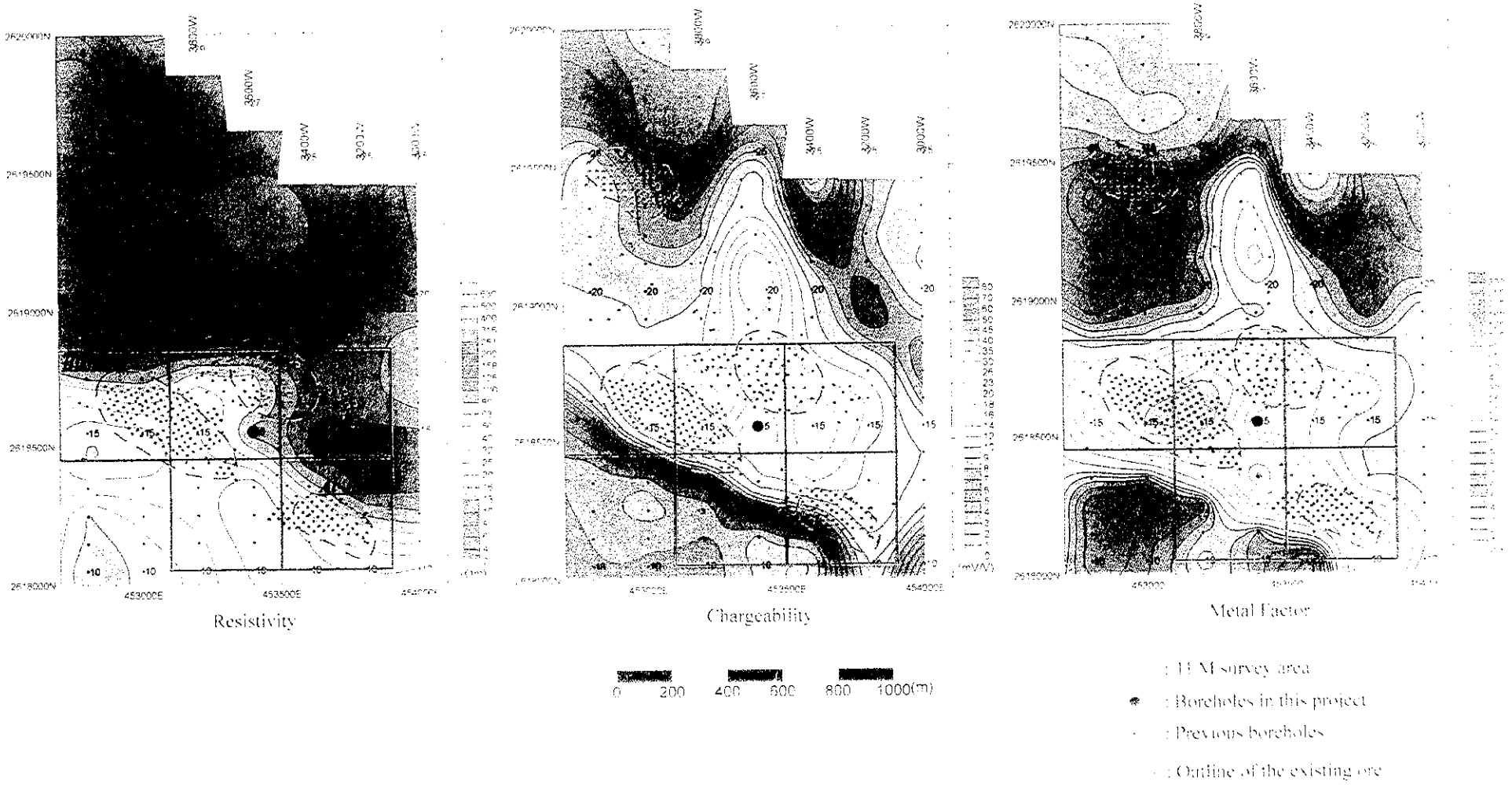

Fig. II-5-26(2) 2D analysis plane maps in Hayl as Safil area at 150m depth

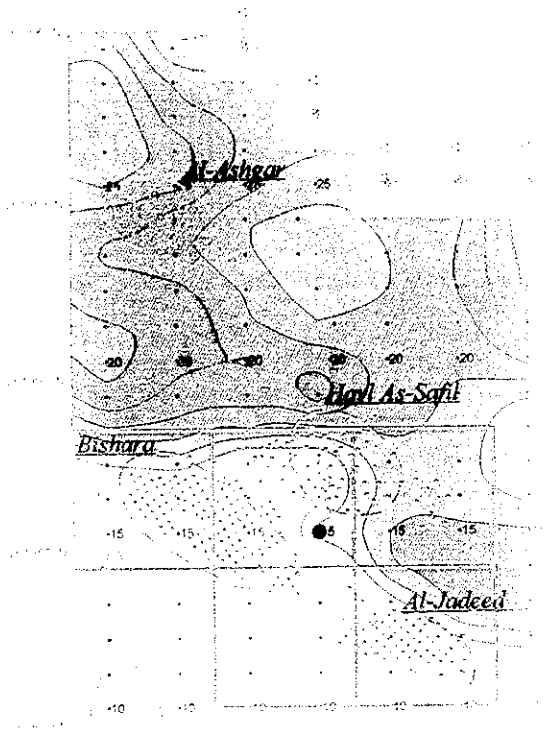

Resistivity

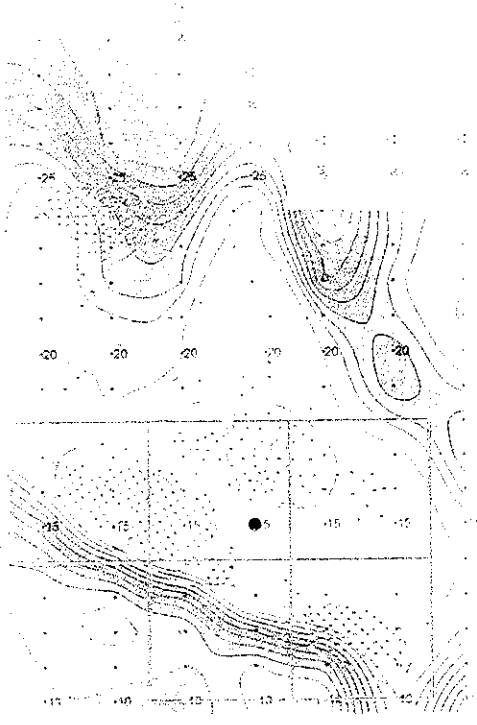

Chargeability

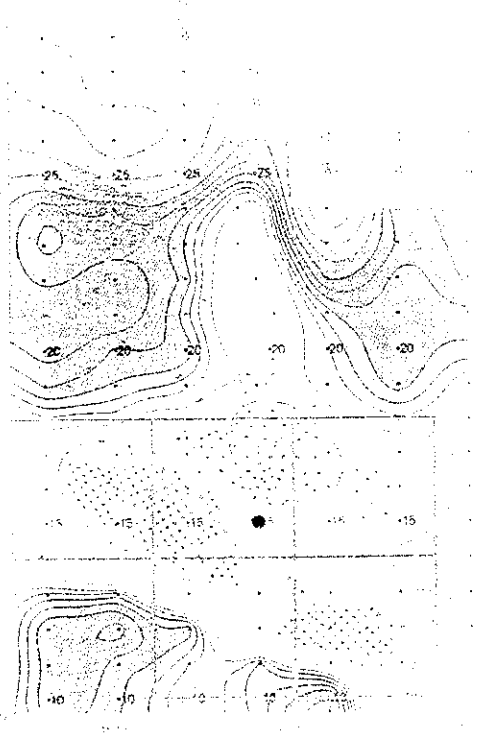

Metal Factor

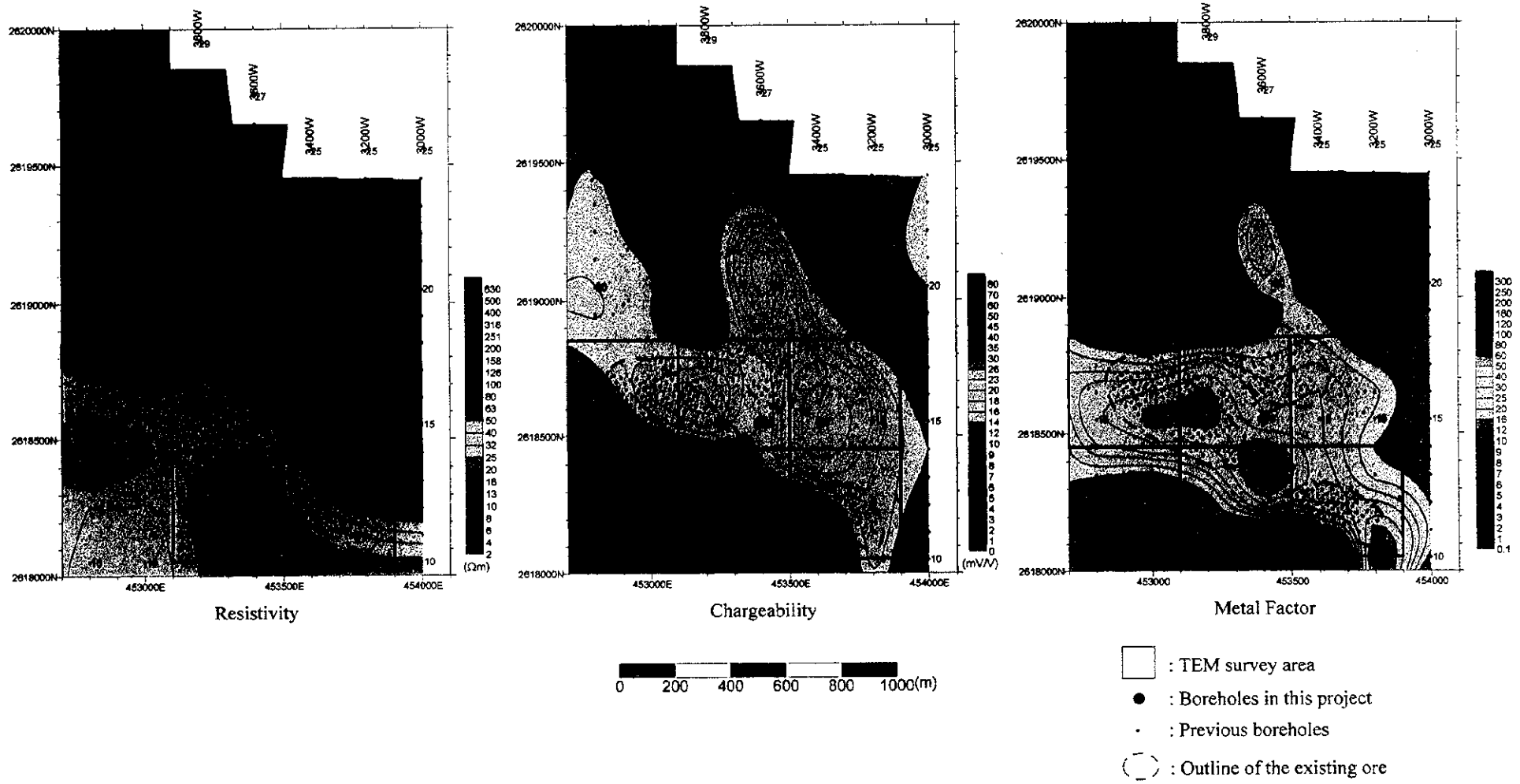

Fig. II-5-26(3) 2D analysis plane maps in Hayl as Safil area at 200m depth

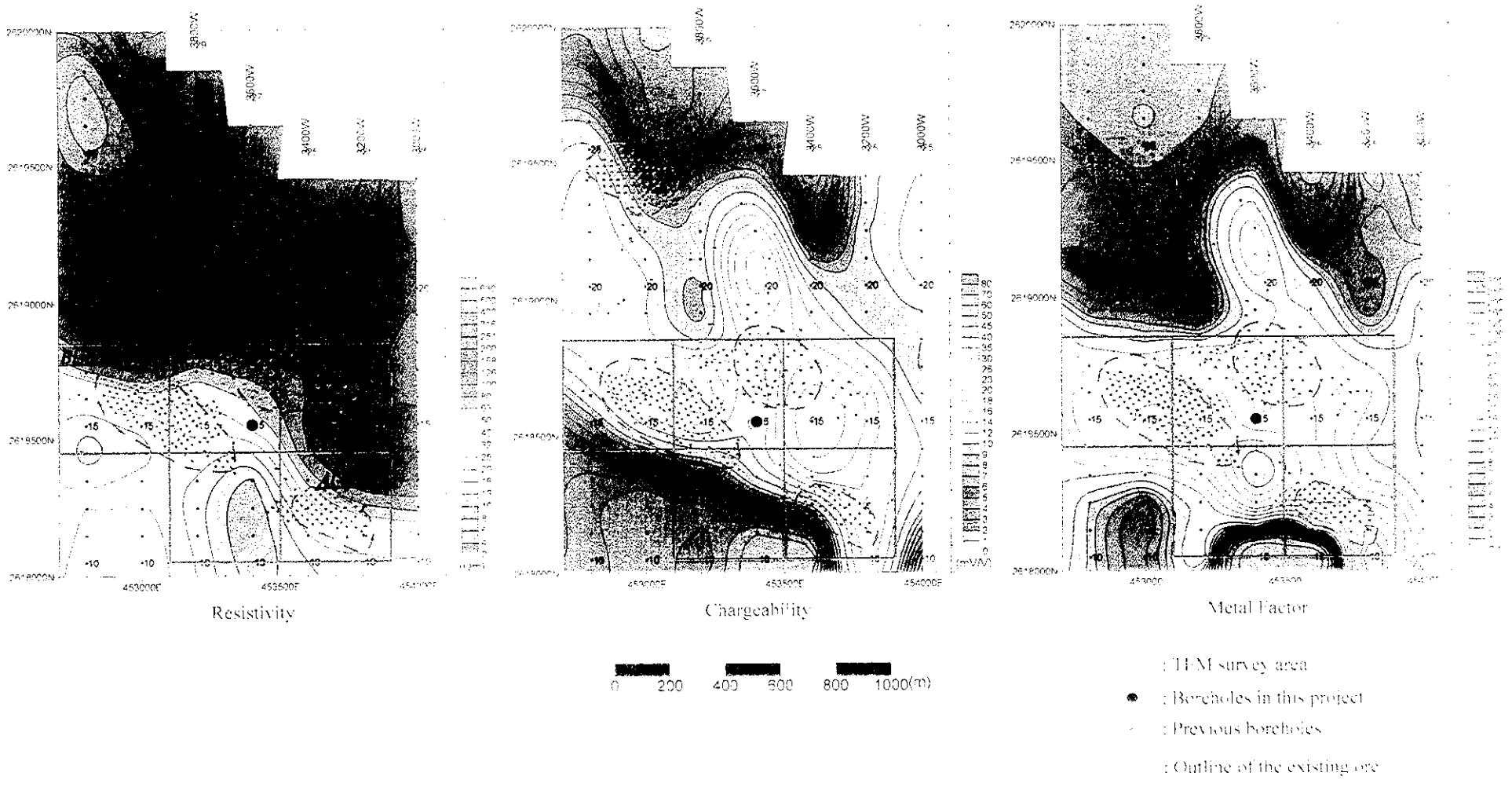

Fig. II-5-26(3) 2D analysis plane maps in Hayl as Safil area at 200m depth

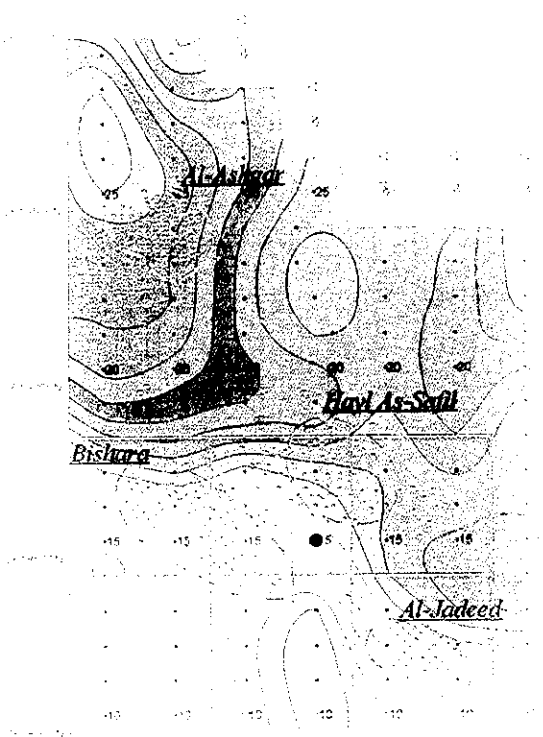
Al-Ashgar
Bisharya
Hawl As-Safil
Al-Jadeed

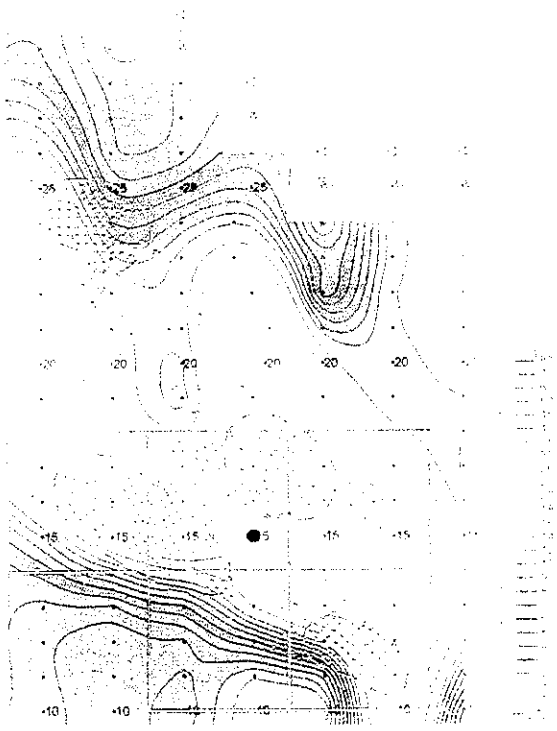

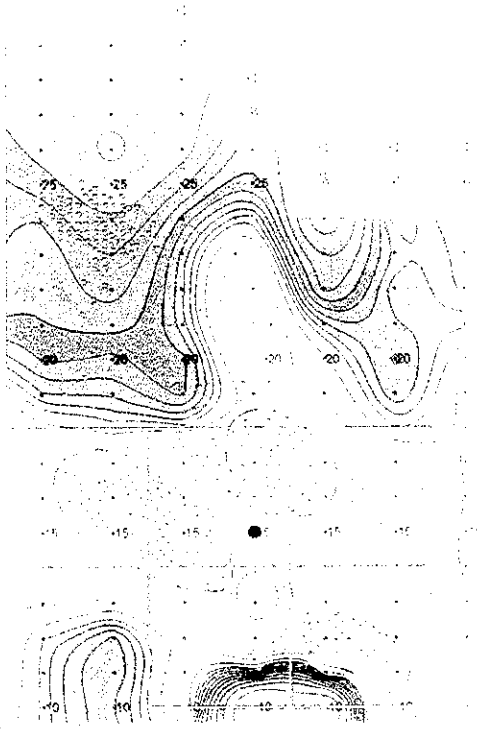

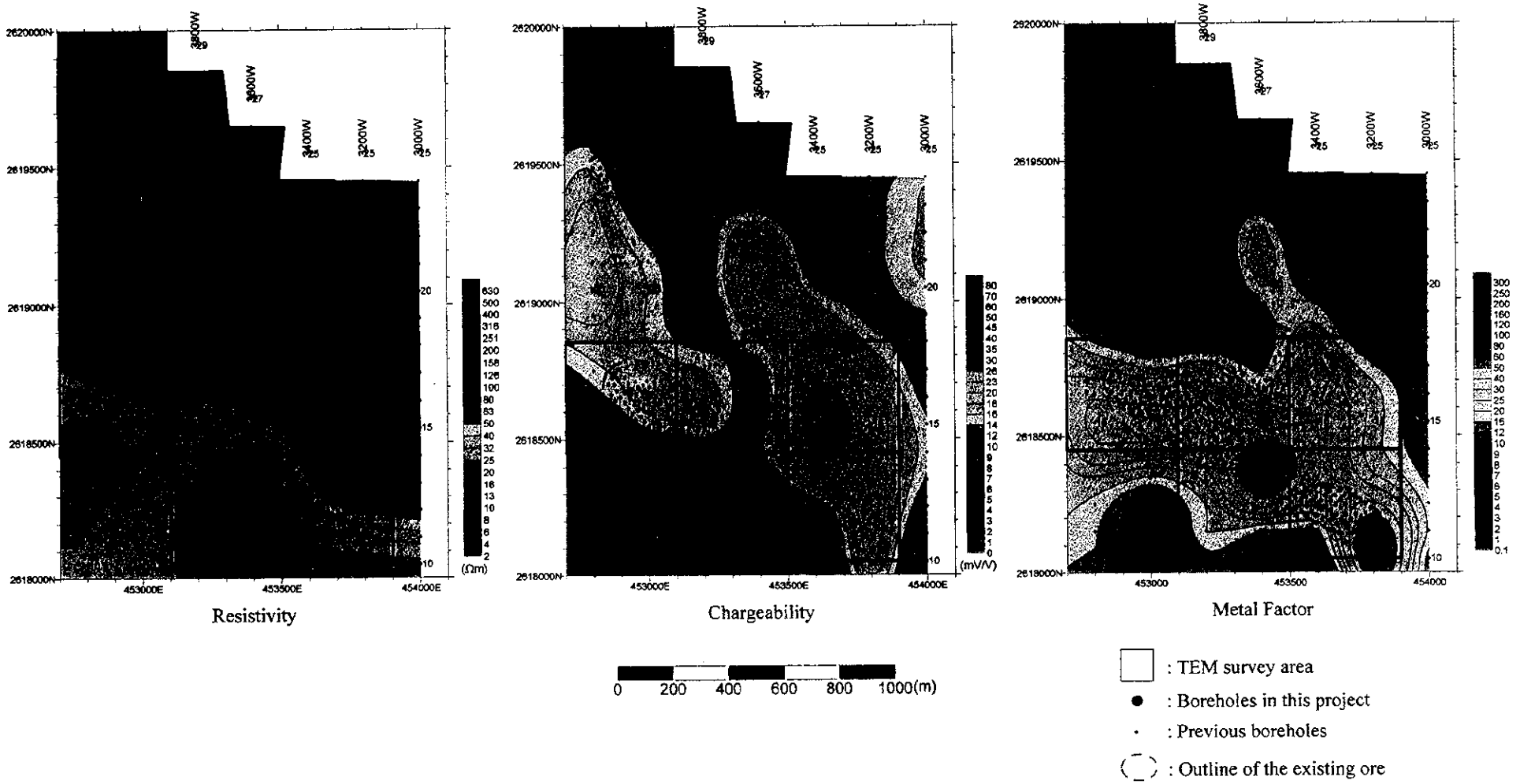

Fig. II -5-26(4) 2D analysis plane maps in Hayl as Safil area at 250m depth

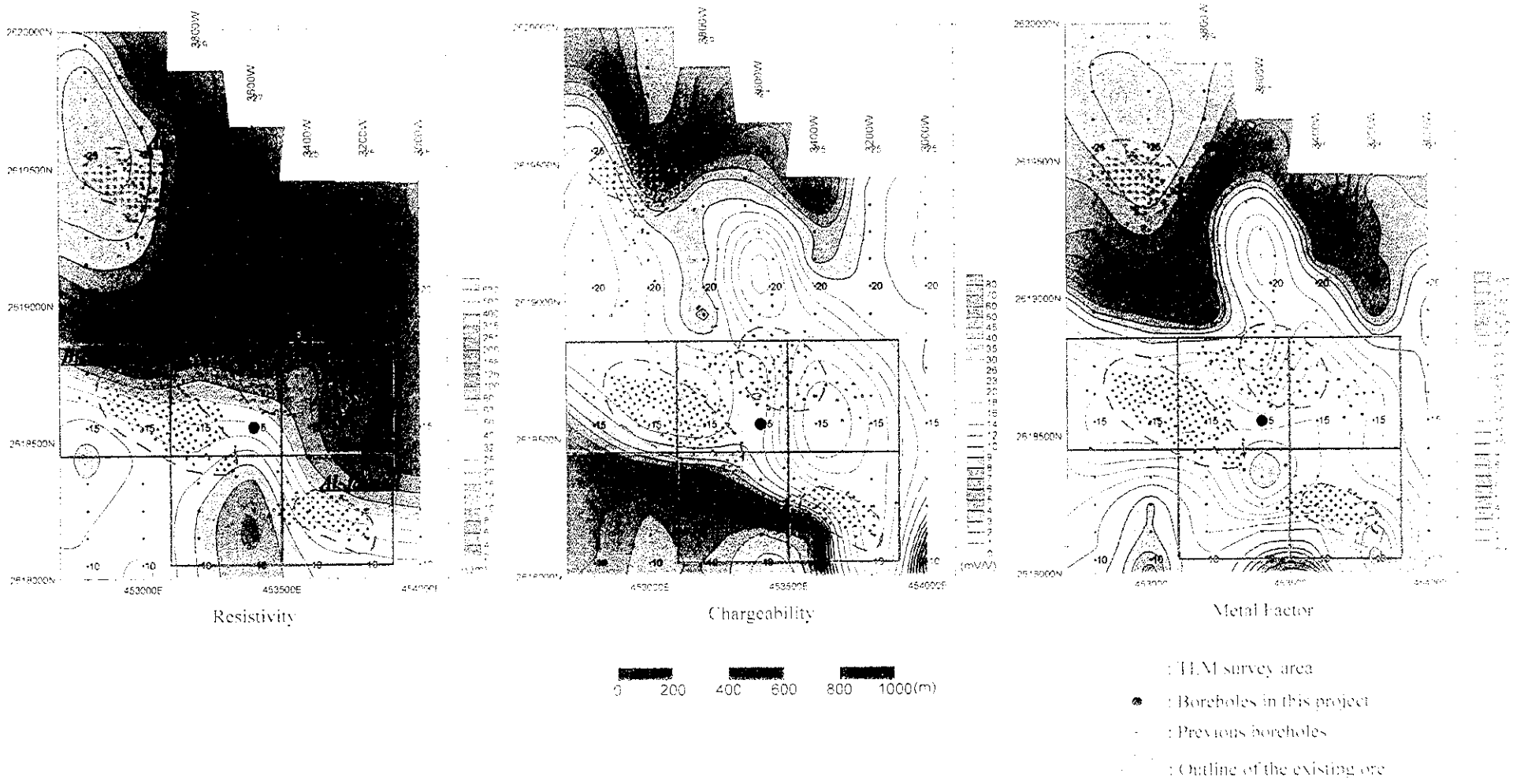

Fig. II-5-26(4) 2D analysis plane maps in Hayl as Safil area at 250m depth

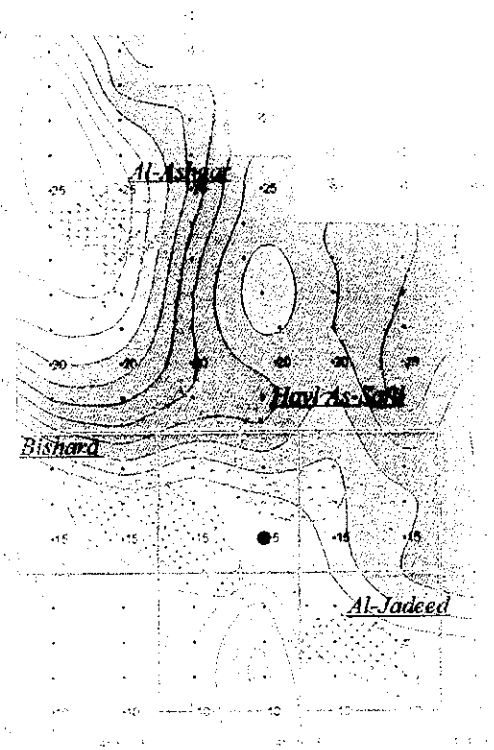

Resistivity

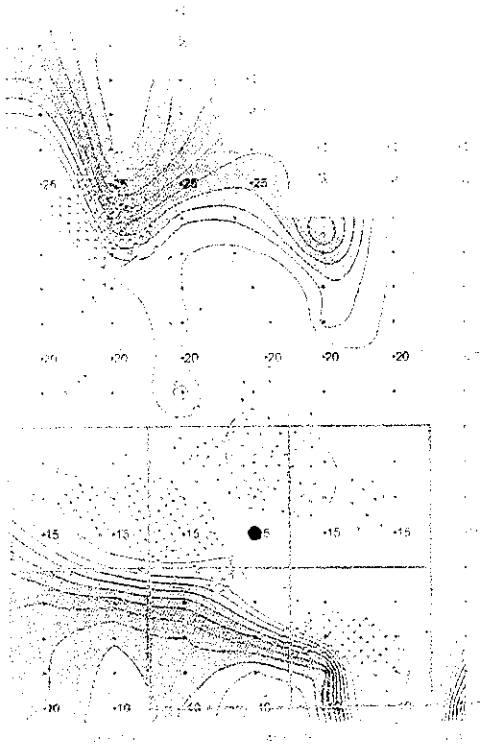

Conductivity

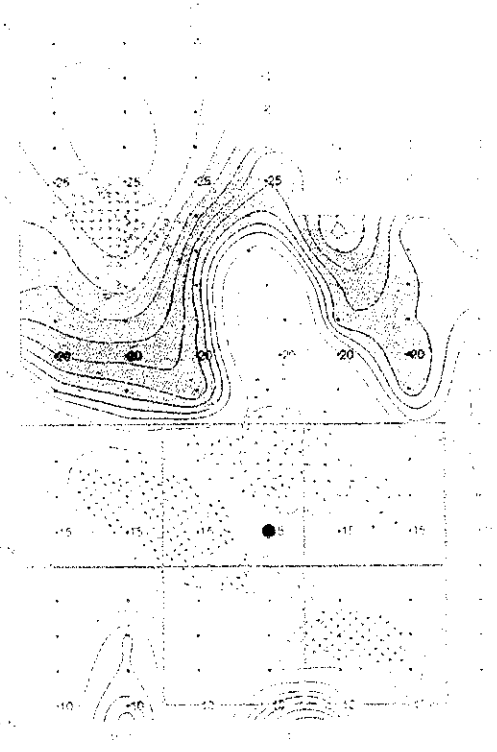

Magnetic

resistivity seen extended to the south may be due to the influence of the low resistivity of the sedimentary rocks which is widely distributed in the southern part, just as in Al Jadeed ore body.

In Hayl as Safil ore body, where the main part is stockwork, remarkable low resistivities are not seen. In N=3,4 in an area centered around the station 500N of the line 3600W, between Bishara and Hayl as Safil ore bodies, high chargeabilities and low resistivities are detected. In this place the possibility of massive sulphide can be inferred, but the resultant pattern may as well be due to the effect of the anomaly that appears due to the influence of Bishara and Hayl as Safil ore bodies and the south part of the sedimentary rocks.

IP anomalies were detected outside of the existing deposit around station 1900N of the line 3600W and near 2200N in the northern part of Hayl as Safil ore body.

According to the results of the 2D analysis, high metal factor is only seen in the shallow part of Al Ashgar and Al Jadeed deposit in agreement with the observed data. In Bishara ore body, resistivity shows low values at N=1,2 while chargeability high values at N=1,4. In Hayl as Safil ore body, whose main ore body is composed of stockwork, resistivity shows entirely high values. In the shallow part of the station 1700N of 3600W, low resistivity values were calculated in agreement with massive sulphide intersected in previous drilling survey. Chargeability shows entirely high values but they become smaller towards depth. Both resistivity and chargeability can be specially seen in the shallow part as a continuous pattern from Bishara ore body to Hayl as Safil ore body, due probably to the shallow depth of ore body. A more detailed 2D analysis of the results is rather limited not only because the depth of ore bodies are shallow and close each other, but also because the interval of 200m between the IP lines and the 100m spaces between the stations results in large grid size for a detailed 2-D analysis.

5-5-5 Najaid area

The 2D results of the TDIP survey carried out in Najaid area and its surroundings are indicated in Fig. II-5-27.

This area is located between Rakah and Tawi Rakah. High chargeability values are distributed within a 200m range along E-W and 100m along N-S, between the lines 1600E to 1800E and at shallow part of 600N to 800N. Due to the high resistivity values detected in this area, the possibility of massive sulphide is rather low but the existence of stockwork evidence better possibilities.

5-5-6 Electrical measurements of rock samples

Representative rock samples from the survey area were analyzed in order to investigate whether the contrast in resistivity between the target mineralization and the volcanic rocks is enough to discriminate between these units in terms of electrical properties.

In general, resistivity and IP measurements in rocks may not reflect in a direct way the intrinsic resistivity or chargeability because of different degree of alteration and water content over the survey area, however clear ideas can be obtained related to the relative variations between rocks units and mineralization.

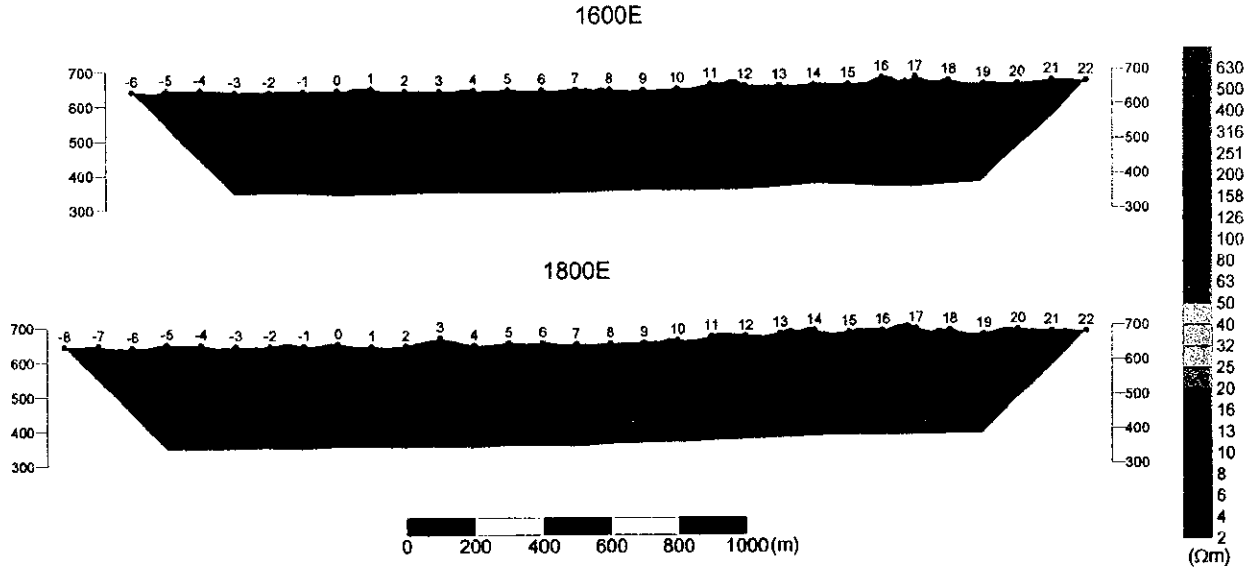

Fig. II -5-27(1) 2D analysis sections for resistivity in Najaid area

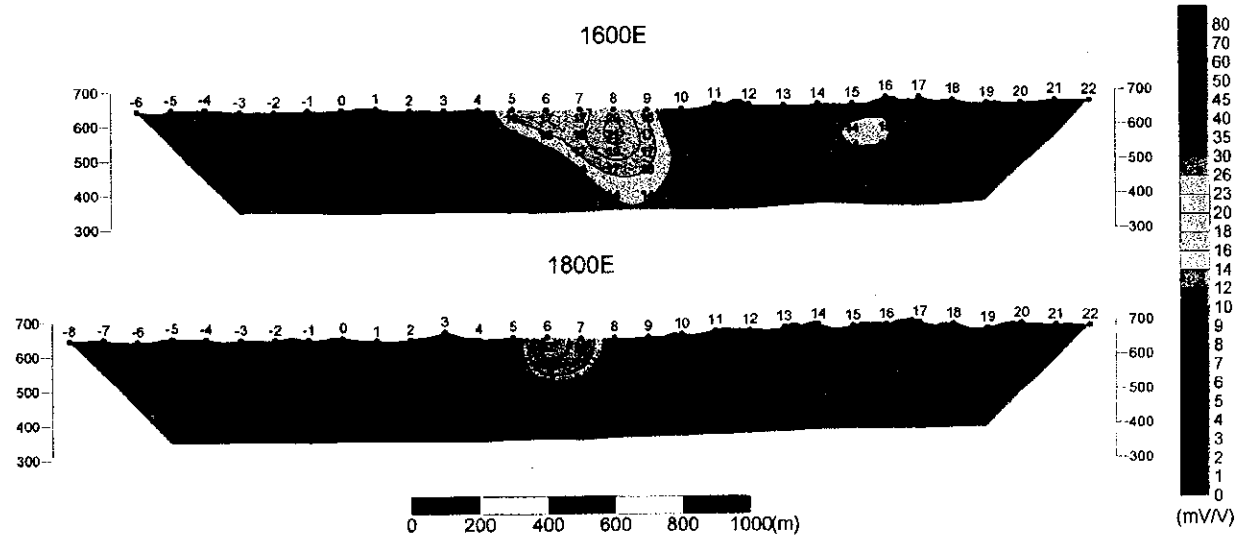

Fig. II -5-27(2) 2D analysis sections for Chargeability in Najaid area

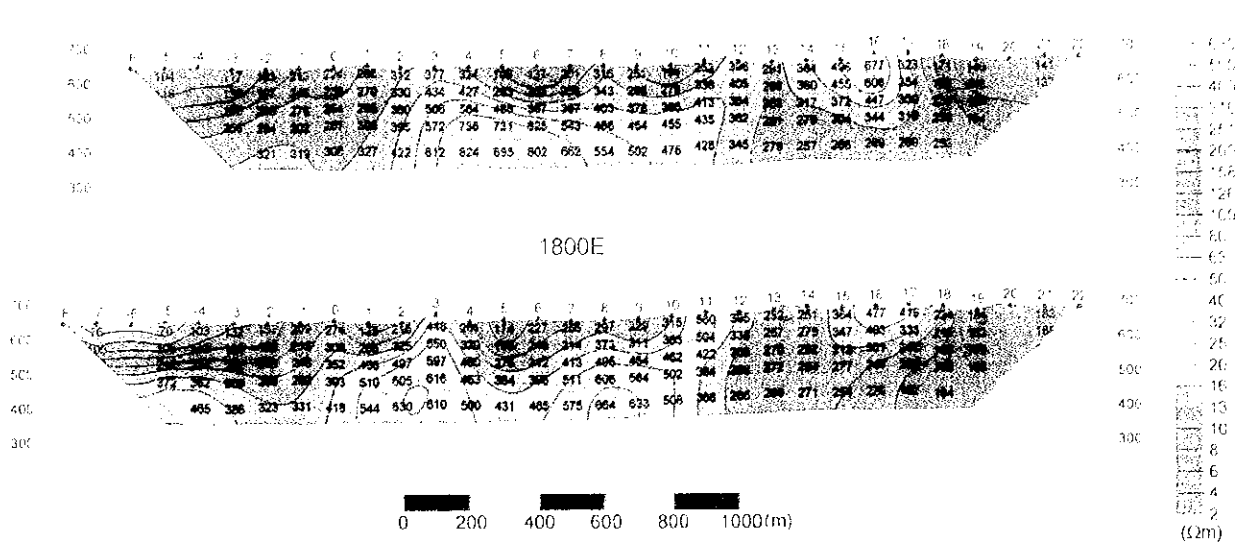

Fig. II -5-27(1) 2D analysis sections for resistivity in Najaid area

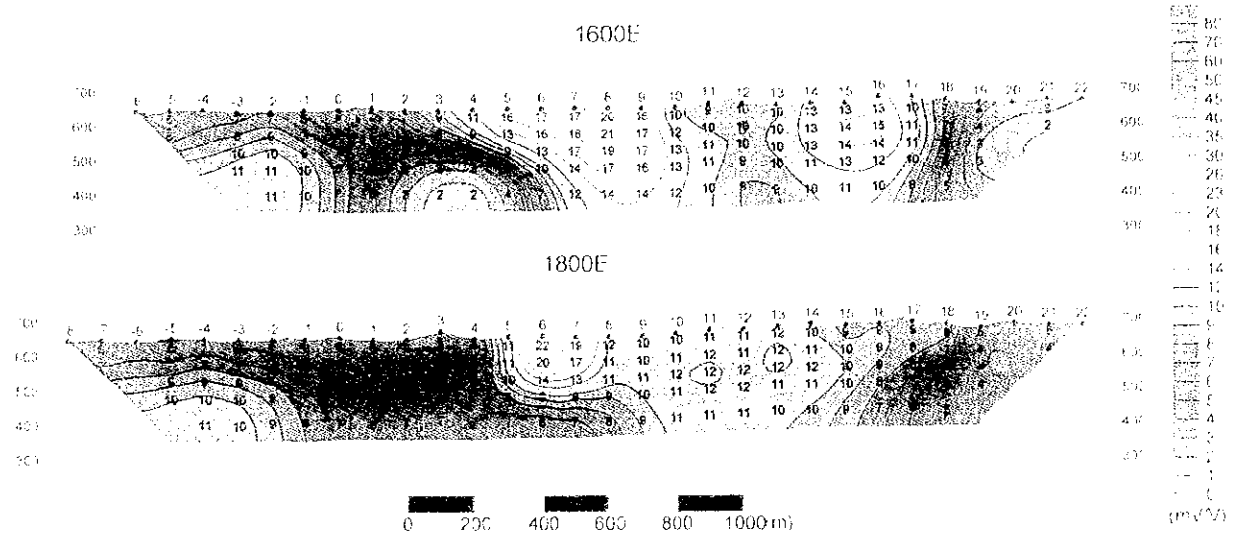

Fig. II -5-27(2) 2D analysis sections for Chargeability in Najaid area

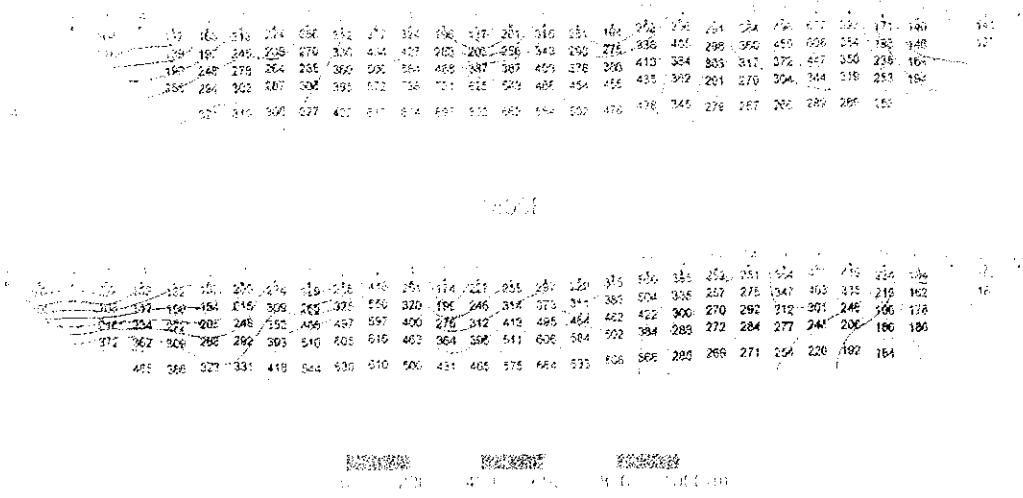

Fig. II-8-27(1) 2D analysis sections for resistivity in Nanaimo area

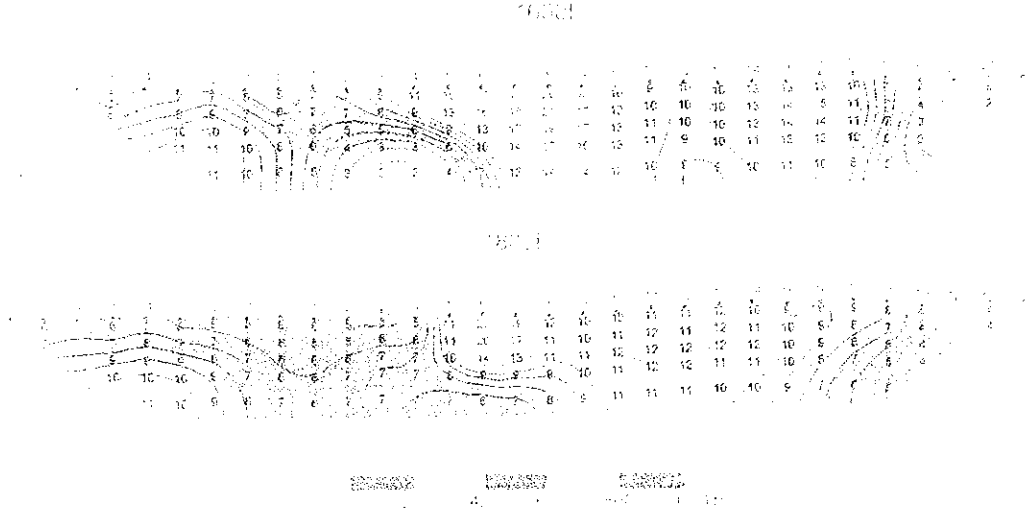

Fig. II-8-27(2) 2D analysis sections for Chargeability in Nanaimo area

(1) Measurement method

Measurement of the electrical properties of rock samples, such as resistivity and IP chargeability were carried out on some samples selected from the survey area. The rock samples were formed into a cylindrical shape and thereafter, soaked into water for a reasonable amount of days but not less than 48 hours. Apparent resistivities as well as chargeability values were measured according to the IP time domain procedures in the laboratory. For this purpose, it was used a Lab Downhole Transmitter LDT-10 made by Zonge. During the determinations of the resistivity and chargeability values, the following formulas were utilized:

For Resistivity:

$$\rho = \frac{A}{L} \times \frac{V_p}{I}$$

where ρ is resistivity (Ωm), A the section of the sample (m^2), L the length of the rock sample (m), V_p the voltage (V) and I the current (A)

For Chargeability:

$$M = \frac{1.87}{V_p} \times \int_{t1}^{t2} V_s dT$$

where M is the chargeability(mV/V), V_p the primary voltage (V), V_s the secondary voltage (mV), dT the sampling interval (sec), $t1$ the off-time voltage 450msec and $t2$ the off-time voltage 1,100msec

(2) Results

Results of the electrical properties of rocks samples measured in the laboratory are indicated in Table Ⅱ-5-2(1) and (2).

The core samples consist of pillow lava and massive lava. Almost all samples show silicification. Many samples include pyrite or chalcopyrite dissemination and vein.

The resistivity values of core samples range from 1.6 to 5k Ωm. Average value is about 1k Ωm. In the case of these samples, the resistivity value depends on the strength of silicification and amount of metallic mineral. In general, strong silicification causes resistivity high and large amount of metallic mineral show low resistivity. The samples No.16 and 19 which include well developed pyrite and chalcopyrite vein show low resistivity value less than 100Ωm. Especially, the sample No.19, in which chalcopyrite vein continues from end to end, show the lowest value 1.6Ωm. The other samples, showing high resistivity above 100Ωm, are influenced by silicification. The resisivity values of stockwork ore samples range between 1.6Ωm and 3kΩm, therefore it is difficult to prospect for stockwork ore on the basis of only resistivity results. The chargeability value depends on the amount of sulphide. The samples which include chalcopyrite vein and stockwork ore samples show high chargeability above 7.5mV/V. The value of the samples in which only pyrite dissemination is recognized range between 1.4 and 7.9mV/V.

Table II-5-2(1) Resistivity and chargeability of rock samples(core)

No.	Borehole	Depth (m)	Resistivity (Ωm)	Chargeability (mV/V)	Rock Name and Formation	Alteration and Mineralization
1	MJOY-2	167.70	4147.0	7.5	Ma (Lasail)	Sili, Py vein & diss (sl)
2		180.75	1713.0	3.3	Pw (Lasail)	Sili, Py vein & diss (sl)
3		195.90	687.2	3.0	Pw (Lasail)	Sili, Epi diss, Py diss (sl)
4	MJOY-3	18.20	139.0	1.5	Ma (Lasail)	Sili
5		65.20	114.8	4.0	Pw (Lasail)	Sili (sl)
6		140.10	132.8	2.4	Pw (Lasail)	Sili, Py vein & diss
7		157.30	120.6	4.3	Pw (Lasail)	Sili, Py vein & diss
8		167.30	145.1	1.4	Pw (Lasail)	Sili, Py diss (sl)
9		189.50	157.7	30.6	Pw (Lasail)	Sili, SW ore, Py-Cp vein, Py diss
10		202.50	223.1	22.3	Pw (Lasail)	Sili, SW ore, Py-Cp vein
11		216.90	798.4	2.6	Pw (Lasail)	Sili, Py diss (sl)
12		225.40	1583.0	14.4	Pw (Lasail)	Sili, Py-Cp vein
13		241.30	836.2	7.5	Pw (Lasail)	Sili, SW ore, Py-Cp vein, Py diss
14	MJOY-5	30.00	341.5	1.3	Ma (Lasail)	Sili (sl)
15		58.85	190.5	4.2	Ma (Lasail)	
16		103.40	56.8	0.5	Pw (Lasail)	
17		131.40	134.6	48.4	Pw (Lasail)	Sili, SW ore, Py-Cp vein, Py & Cp diss (sl)
18		170.15	265.5	2.6	Pw (Lasail)	Sili, Py diss (sl)
19		208.20	13.4	149.1	Pw (Lasail)	Sili, Cp vein, Py diss (sl)
20	MJOY-6	24.95	5225.0	7.9	Pw (Lasail)	Sili, Py diss (sl)
21		73.60	2525.5	5.2	Pw (Lasail)	Sili, Py diss (sl)
22		152.80	1.6	75.1	Pw (Lasail)	Sili, SW ore, Py-Cp vein, Py diss (sl)
23		176.80	1606.0	3.4	Pw (Lasail)	Sili, Py vein, Py diss (sl)
24		222.80	3172.5	8.7	Pw (Lasail)	Sili, SW ore, Cp vein, Py diss (sl)
25	MJOY-7	26.00	99.0	2.4	Pw (Lasail)	Sili (sl), Py vein, Py diss (sl)
26		83.95	856.4	7.1	Ma (Lasail)	Sili (sl), Py vein, Py diss (sl)
27		117.45	1509.5	9.4	Pw (Lasail)	Sili (sl), Py-Cp vein
28		183.10	541.4	3.3	Pw (Lasail)	Sili (sl)
29		215.20	2570.0	5.0	Pw (Lasail)	Sili (sl), Py diss(sl)
30		249.10	501.0	2.4	Pw (Lasail)	Sili (sl)

Remarks

Ba: Basalt
Pw: Pillow lava
Ma: Massive lava
Do: Dolerite

Cp: Chalcopyrite
Py: Pyrite
Ca: Calcite
Epi: Epidote
Qz: Quartz
Sili: Silicified
SW: Stockwork
diss: dissemination
vein: veinlets
(sl): Slight

Table II-5-2(2) Resistivity and chargeability of rock samples(outcrop)

No.	Sample Name	Location (UTM)	Resistivity (Ωm)	Chargeability (mV/V)	Rock Name and Formation	Alteration and Mineralization
31	YN01	459800E 2617750N	974.2	7.3	Basalt(Lasail unit); Massive lava, light green.	silicified
32	YN02	459800E 2618400N	5169.3	3.5	Dolerite(dike in Lasail unit), light green.	silicified
33	YN03	460000E 2616500N	3287.3	2.3	Basalt(Lasail unit); lava, greenish gley.	
34	YN04	460000E 2618250N	492.0	2.5	Mudstone(Lasail unit); metalliferous sediment, reddish brown.	
35	YN05	460200E 2616750N	8107.8	2.0	Andesite(Lasail unit); pillow lava, light gley.	
36	YN06	460400E 2615050N	474.9	5.2	Basaltic andesite(Alley unit); lava, dark gley.	
37	YN07	460400E 2618424N	1720.3	2.5	Dolerite(Sheeted dike), light green.	similar to YN03
38	YN09	456600E 2617300N	8071.5	3.2	Limestone; magnetic, black.	
39	YN10	456400E 2616650N	18.3k, 9.8k, 38.6k	8.8, 4.3, 7.1	Limestone; gley	
40	YN11	456200E 2617750N	49.4k, 12.7k, 6.9k	7.6, 1.1, 1.0	Limestone; white	
41	YN18	455200E 2618300N	11.2k, 4.9k	2.6, 1.0	Gabbro	
42	YN27	458940E 2615827N	653.2	0.3	Basaltic andesite(dike in Alley unit), light green.	silicified

The chargeability values of core samples range from 0.5 to 149.1mV/V eit an average value of 14.7mV/V.

Outcrop samples consist of basalt, andesite, gabbro, mudstone and limestone.

Outcrop samples show generally high resistivity values ranging from 479.9Ωm to 50kΩm. Especially, limestone and gabbro show high values above 10k Ωm. Limestone shows anisotropy.

The chargeability values of outcrop samples range from 0.3 to 8.8mV/V. Except the samples No.31, 36, 39 and 40, the values are less than 4mV/V. The high chargeability values of No.31 and 36 are caused by clay minerals. The high values of No.36 and 39 are caused by magnetite. Limestone shows anisotropy.

5-6 Further Considerations

High chargeability distributions due to mineralization were detected in five places. Though massive sulphide was not detected, promising stockwork ore was intersected at Quron Al-Akbahb anomaly area. In Hayl as Safil area, IP anomaly due to ore body found by previous survey was detected. Small scale massive sulphide like as Al Ashgar or Al Jadeed ore body is clearly detected as low resistivity and high chargeability zone, so it is certified that TDIP method is useful for prospecting for massive sulphide ore. In Quron Al Akhbab area, as the results of TDIP, TEM and drilling, we can understand that stockwork shows high chargeability and medium to high resistivity. Existence of sotckwork ore is expected at the south-east part of the open pit of Rakah mine and Najaid area, because high chargeability and middle to high resistivities are distributed at these areas.

CHAPTER 6 TEM SURVEY

6-1 Background and Objectives

The TEM (Transient Electro-Magnetic) survey, sensitive to conductive bodies, such as massive sulphide deposits, was conducted to clarify the nature of the sulphide mineralization within the area delineated by the results of the TDIP survey.

During the present survey, large fixed loops were located within the anomalies extracted from the TDIP survey. Because of the remarkable responses given by conductive materials, such as massive sulphide ores, this detailed method is useful to extract ore bodies and to estimate their locations and boundaries.

6-2 Survey Locations and Specifications

The TEM method was utilized in the Yanqul region by using large fixed loops of 600m by 600m. In relation to the amount work undertaken during the TEM survey and as indicated in Table II-6-1, a total of 7 loops corresponding to 567 stations were carried out this year.

Table II-6-1 Survey amounts of TEM

Area	Number of Loops	Number of Points
Rakah Gold Mine	1	81
Quron Al Akhbab	1	81
Hayl As Safil	5	405
Total	7	567

6-3 TEM Survey Method

6-3-1 Basic principles

The principle of the TEM method used in this survey is to energize an ungrounded loop situated on the surface of the earth, as illustrated in Fig. II-6-1. When the currents flowing in the loop are switched off, free electron conduction currents are induced (eddy currents) in the ground. The characteristics of the eddy currents are known to depend on the conductivity, size, and shape of the conductive body, and position with respect to the sending loop. These eddy currents set up a secondary magnetic field, which can be detected by a receiver coil as a time-dependant decaying voltage. The measurement of the time dependent decaying voltage is a means of detecting conductors in the ground. This transient decay can be measured by a number of measurement channels recording the voltage at

various delay times after the transmitted fields are switched off. According to Faraday's law, the quick shut-off of the primary magnetic field caused by the current termination induces a pulse of e.m.f. (voltage) in the surrounding media. The resulting eddy currents produced in nearby conductive material support a surrounding secondary magnetic field for the duration of the pulse. Thereafter, with no external e.m.f. to support it, this system of currents and magnetic field decays with time, and it is this transient magnetic field that the receiver measures. These measurements occur during fixed time "windows" which occupy most of the "off-time" of the transmitter. As the receiver must know when the transmitter is off, synchronization was done by using crystal clocks.

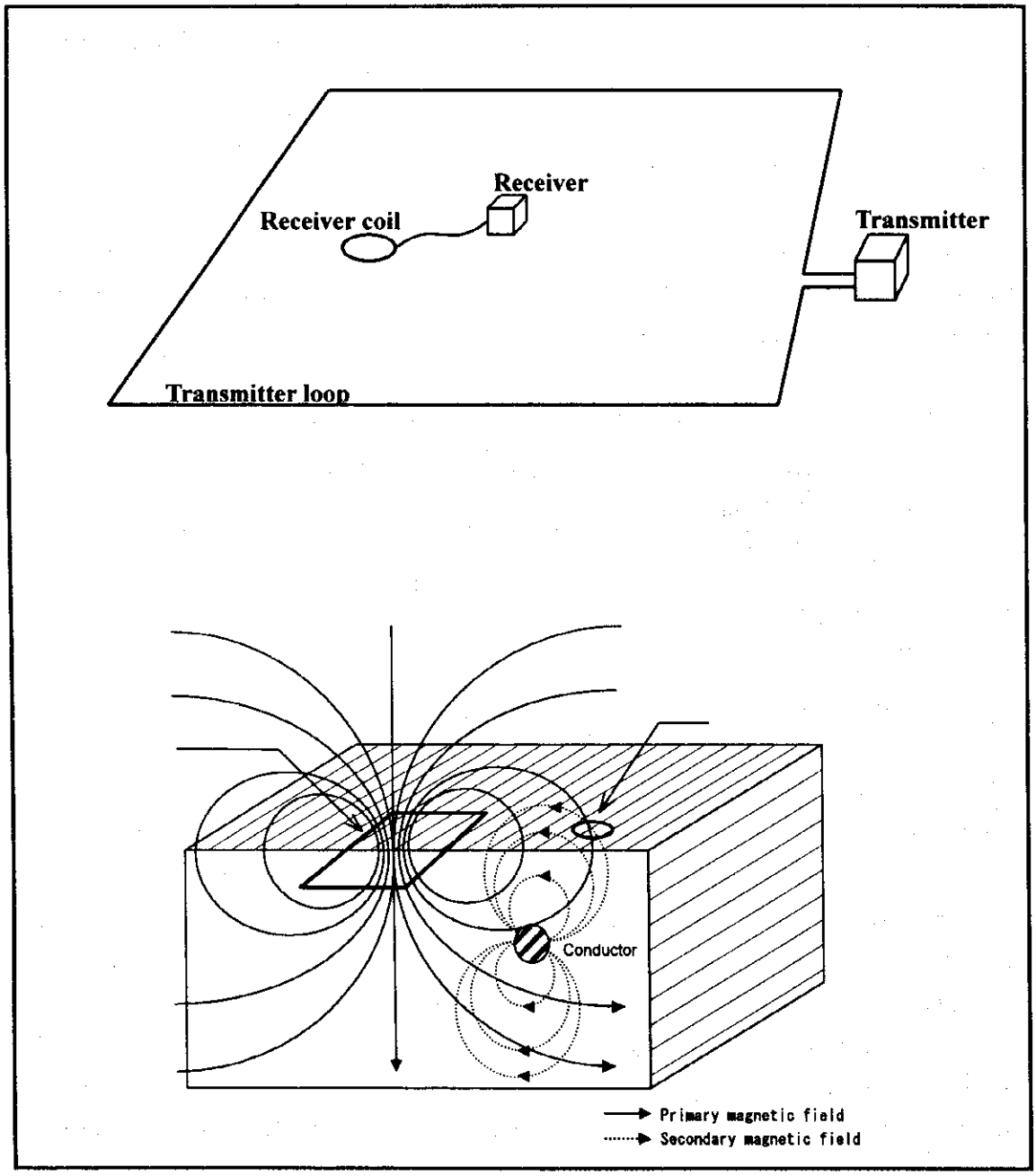

Fig. II-6-1 Schematic TEM survey configuration

6-3-2 Logistics and data acquisition

There are several varieties of TEM systems and modes of operations. During this survey, the configuration of large fixed-loop was used. For the case of large loops, a large, single-turn square loop of wire of 600m by 600m is laid out on the ground. A portable power generator of 2500W fed a transmitter, which provides a series of alternating bipolar currents pulses with slow exponential turn-on and a rapid linear turn-off precise current waveform through the loop. After the transmitter loop has been set up, a small portable multi-coil receiver is moved to stations along surface lines inside the loop. Lines were surveyed within the loop to a distance of 100m away from the loop and the grid interval between the observed points was 50m.

Previous to the data acquisition, the crystals of the transmitter and receiver are warmed up before attempting to synchronize. Synchronization of the transmitter and receiver was carried out using the built-in high stability quartz crystal oscillators. Integration for each measurement was carried out over 2^8 cycles.

The current waveform driven through the transmitter loop and the number of spacing of channels in the receiver are the main distinguishing features of this method. 20 time channels with locations and widths are shown in Table Ⅱ-6-2. Successive operations at 25Hz, then 2.5Hz, effectively gives 30 channels covering range from 88μsec. to 72 msec. A steady current is terminated rapidly by a 220μsec. ramp in large loops.

During data collection, several transient decays are recorded for each sounding. Readings are acquired at several receiver gains with opposite receiver polarities for each sounding location to eliminate any cultural noise. Many pulses of positive and negative polarities are stacked in a short period of time and averaged to remove any disturbance. Fig. Ⅱ-6-2 shows example of decay curve.

Table Ⅱ-6-2 Channel times after switch off

Channel Number	Sampling Time (μsec)	Window Width (μsec)
1	88	18
2	107	24
3	131	36
4	162	37
5	201	40
6	251	72
7	314	76
8	396	100
9	499	142
10	631	156
11	799	180
12	1014	250
13	1287	380
14	1636	390
15	2081	500
16	2648	720
17	3373	780
18	4297	1080
19	5475	1420
20	6978	1560

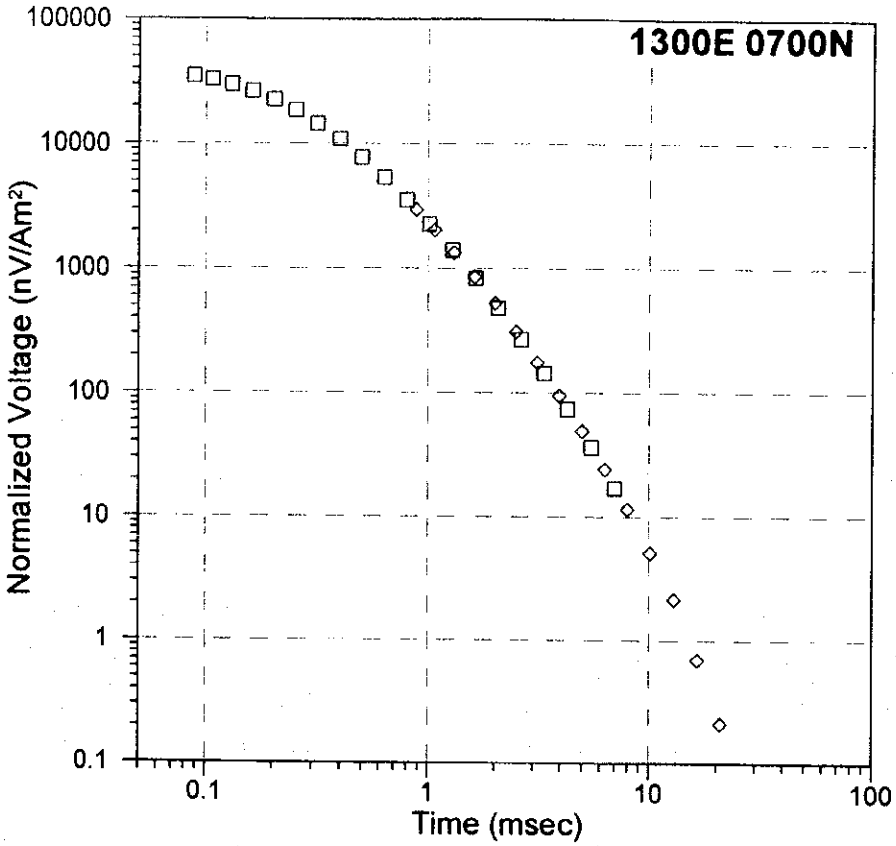

Fig. II -6-2 Example of TEM decay curve

6-3-3 Equipment specifications

The EM37 system manufactured by Geonics Ltd. of Canada was utilized during the TEM survey of this year with the specifications as detailed in Table II -6-3. The receiver used is the Protem.

The current waveform in the transmitter consists of alternating bipolar current pulses with a slow exponential turn-on and a rapid linear turn-off. The base frequency of operation can be set at 2.5, 6.25 or 25 Hz, with corresponding window times of 71.9, 28.7, or 7.17 msec respectively. In this survey we used a base frequency of 25 Hz.

Table II -6-3 Specifications of TEM survey instruments

Items	Specification
Transmitter : EM37	Max output:30A,180V
Generator : GPU2000	5HP,120V,3phase,400Hz
Receiver : PROTEM	25Hz: 0.088-7.19ms
	6.25Hz: 0.35-28.7ms
	2.5Hz: 0.88-71.9ms
Magnetic Sensor	Induction Coil
	Effective area $100m^2$

At the receiver the induced voltage in the coil is measured in millivolts. Using the effective area of the coil and the gain of the receiver, these measurements are converted to the time derivative of the magnetic field in nanovolts/amp-meter^2.

6-4 Analysis Method

The fact that the primary field is absents during measurement time, leads to "cleaner" data that is easier to interpret. The rate of decay of a conductor's magnetic field depends primarily on its size and conductance. Eddy currents decay rapidly in poor conductors, while those due to good conductors decay slowly, and the timing of the channels is such that only the effects of eddy currents due to the good conductors are seen in the later channels. In conductive environments, therefore, the response from overburden and weak mineralization should be minimal in the later channels where the target response predominates.

The first step in data processing is to average the e.m.f. (voltages) that are recorded at opposite receiver polarities. Then, the records at different amplifier gains are combined to give a single composite transient decay. After the composite transient decay has been calculated for each measurement point, the late stage apparent resistivities are calculated by using the following equation:

$$\rho_a(t) = \frac{\mu^{5/3} M_r^{2/3}}{20^{2/3}\pi} \cdot \frac{M_t^{2/3}}{t^{5/3} V^{2/3}}$$

Where V is the voltage measured at the receiver, M_r is the moment of the receiver, M_t is the moment of the transmitter, μ is magnetic permeability, and t is the time measured after transmitter switch off.

The TEM response detected in the receiver, depends not only on the electrical properties of the ground, but also on the location of receiving points and transmitter loop size, generally the highest response are observed at the center of the loop. To correct the response due to the receiving location, the following procedure was carried out:

A layered resistivity structure was calculated by 1D inversion analysis using the data at the center of the loop. We assumes that this electrical structure represents an average resistivity in the loop.

By using the parameters of this resistivity structure, a synthetic response $Bc(x, y)$ was calculated at all the points within the loop by taking also into account the relative position between the receiver and transmitter loop. If the resistivity structure at a point is nearly same as the average resistivity structure, the observed EM response should be almost the same as the calculated synthetic response, resulting in a minimal difference. On the contrary and if the average resistivity structure is not related to an anomaly but the point represents the location of the conductive body underlied, then the response becomes extremely high as compared with the synthetic response, and therefore, the difference between the responses becomes high, i.e.,

$$\Delta B(x, y) = \log(Bo(x, y) / Bc(x, y))$$

Where: $\Delta B(x, y)$ is the difference of response, $Bo(x, y)$ is the observed response, $Bc(x, y)$ is the synthetic response, and log is the logarithm of base 10 (Fig. II-6-3).

Contour map of the difference in the TEM responses permit the clarification of anomalies (if any) by the contrast in the TEM response values.

For the depth estimation, the following formula is used:

$$d = \sqrt{500 \rho t}$$

Where ρ is the average resistivity(Ωm), t is the time(msec) and d is the depth(meter)

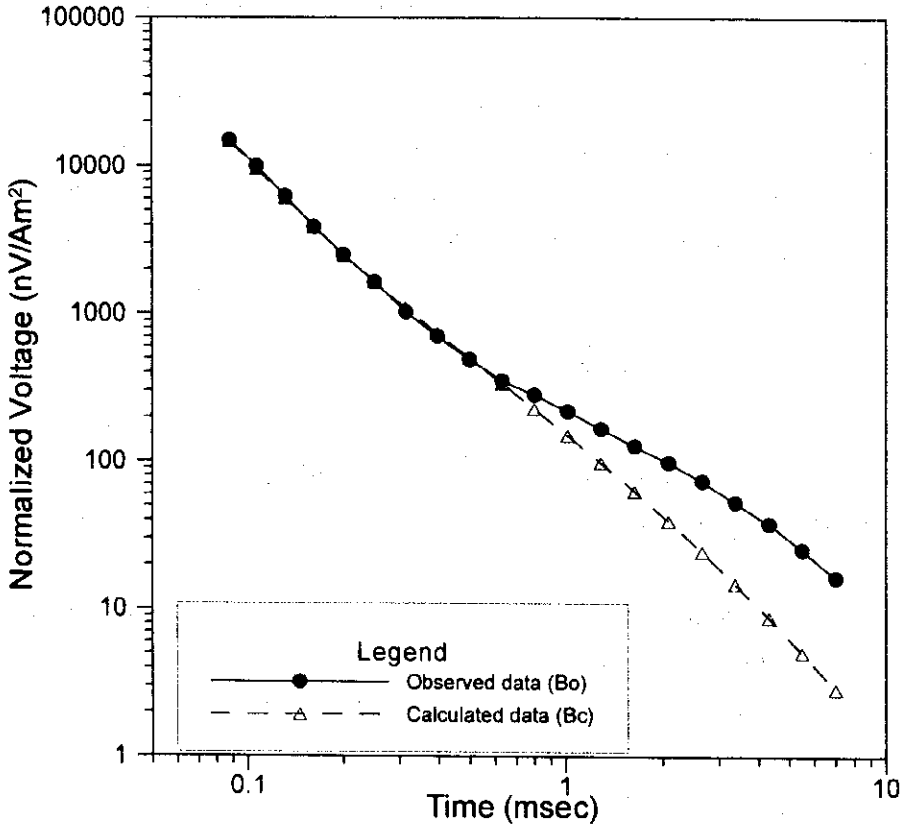

Fig. II-6-3 Observed and background TEM responses

6-5 Survey Results

Table II-6-4 indicates the estimated exploration depth based on the above mentioned formula. Since these values are calculated for a layered structure at the center of the loop, the calculated depth should be taken with caution because it does not always correspond to the real depth.

Table Ⅱ-6-4 Depth estimation in survey area

Channel	Rakah Gold Mine	Quron Al Akhbab	Hayl Al Safil				
	Loop-1	Loop-2	Loop-3	Loop-4	Loop-5	Loop-6	Loop-7
Ch-01	112	124	33	46	33	37	35
Ch-02	125	139	37	51	37	41	39
Ch-03	142	157	41	58	42	46	44
Ch-04	160	176	47	65	47	52	50
Ch-05	178	197	52	73	52	58	56
Ch-06	201	222	59	83	59	66	63
Ch-07	226	250	66	93	67	74	71
Ch-08	253	279	74	104	74	83	79
Ch-09	285	315	83	117	84	93	89
Ch-10	320	353	93	131	94	105	100
Ch-11	353	390	103	145	104	116	110
Ch-12	394	435	115	162	116	129	123
Ch-13	447	493	130	183	132	146	139
Ch-14	503	556	147	206	148	165	157
Ch-15	562	621	164	231	166	184	175
Ch-16	635	702	185	260	187	208	198
Ch-17	714	789	208	293	210	233	223
Ch-18	798	881	233	327	235	261	249
Ch-19	900	994	263	369	265	294	281
Ch-20	912	1118	295	415	298	331	316

6-5-1 Rakah Gold Mine anomaly

(1) Loop location

A TEM survey was carried out by setting a large fixed loop on the high chargeability anomaly detected from the TDIP survey carried out around the Rakah open pit. Fig. Ⅱ-5-4 illustrates the location of the 600m by 600m transmitter loop indicating the places where the IP anomalies were detected.

(2) Results

Loop 1

To process the data, a background response was stripped from the original field response (observed data). The data was processed by subtraction from a two-layer earth (host rock) response. The host rock response was calculated from the following model:

- An upper layer of 130 Ωm, 250m thickness
- A basement layer of 400 Ωm.

Fig. Ⅱ-6-4(1) and Fig. Ⅱ-6-4(2) show the TEM responses obtained at different channels, i.e. from

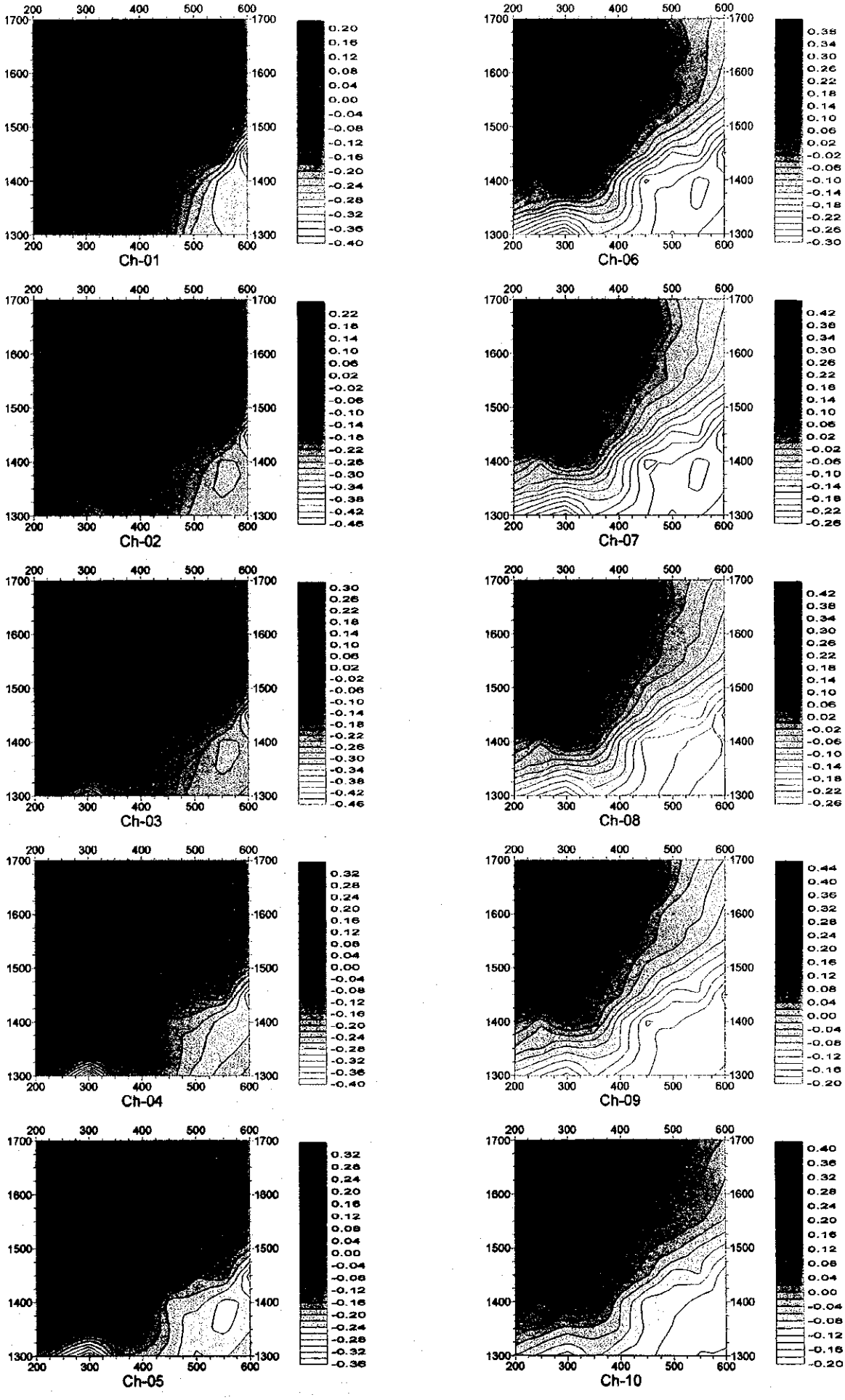

Fig. Ⅱ-6-4(1) TEM response maps of Loop1 (Ch1-Ch10)

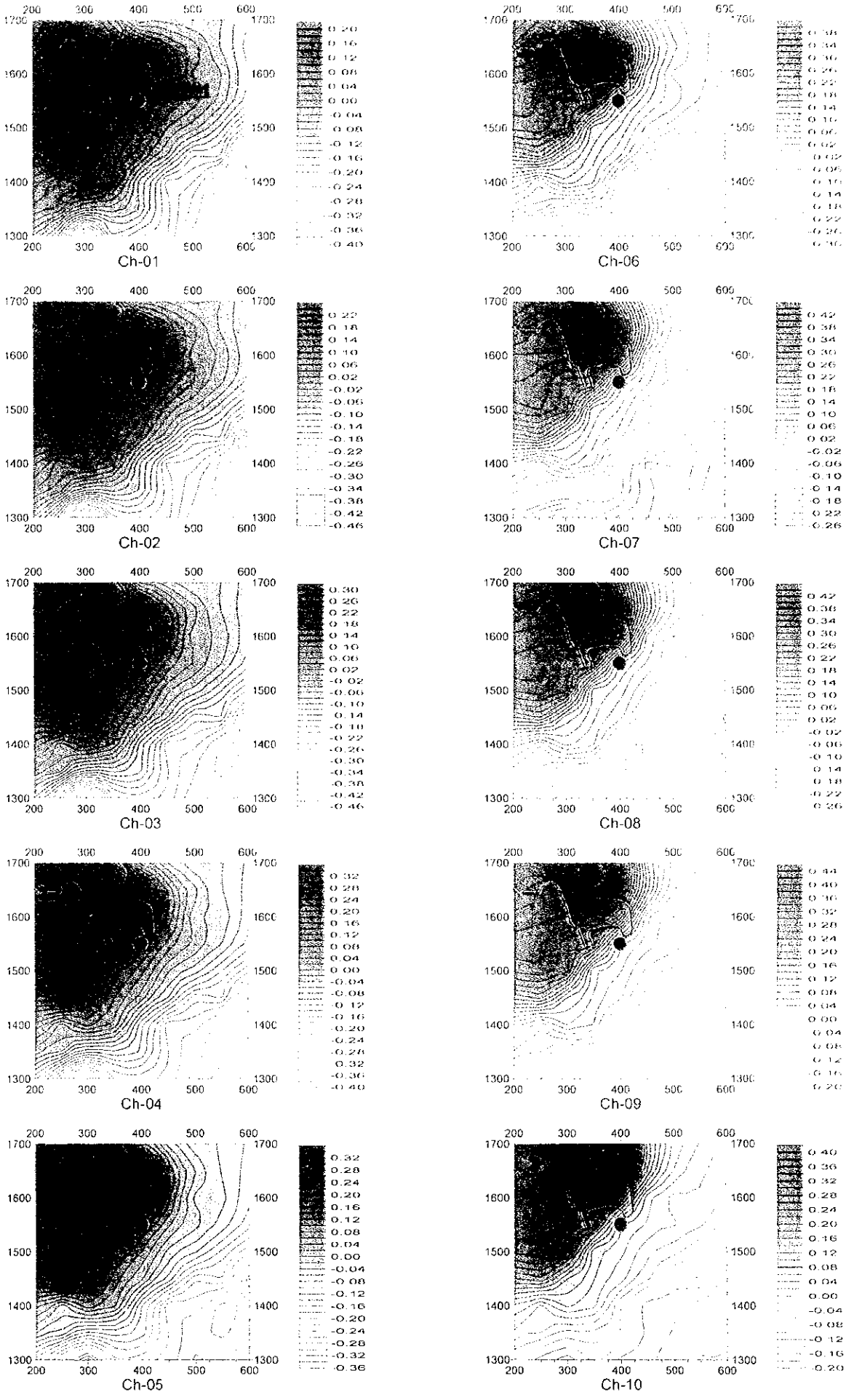

Fig. II-6-4(1) TEM response maps of Loop1 (Ch1-Ch10)

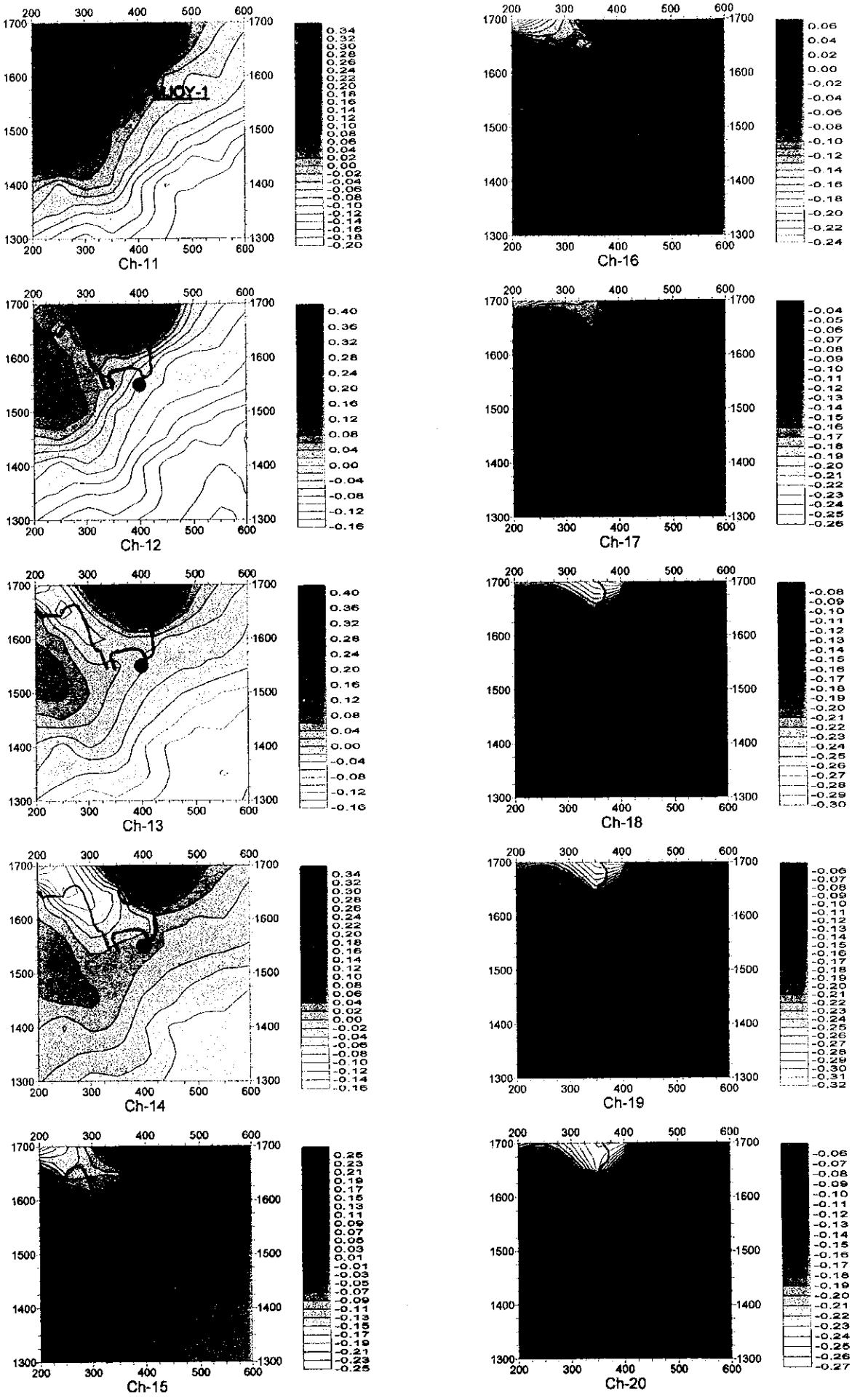

Fig. II -6-4(2) TEM response maps of Loop1 (Ch11-Ch20)

channel 1 to channel 20.

A high TEM response is seen widely distributed around the NW part of the loop in agreement with the relatively low resistivity indicated by the TDIP survey from shallow to intermediate levels (N=1,2). At deeper levels a somewhat high TEM response is distributed around the central part of the loop along NE-SW direction in agreement with a relative low resistivity zone detected by TDIP at N=4. To study the nature of this anomaly the borehole MJOY-1 was drilled at the station 400E, 1550N.

A small negative response was obtained around the stations 1700N, 300E and 1700N, 400E. This response that occurred at intermediate channels may have been probably caused by the dependence of the conductivity of the ground with frequency. This information was not utilized during the data processing.

The TEM survey shows that the resistivity results, as calculated by the TEM response, are not representative of a conductive deposit and therefore a clear EM signature was not clearly defined by the TEM method. The resistivity characteristic measured by the TDIP method did not either indicated high values.

6-5-2 Quron Al Akhbab anomaly

(1) Loops location

Quron Al-Akhbab as indicated in Fig. II-5-4 as Loop-2, is located about 3km east of Rakah Gold Mine.

The TEM survey was carried out on the basis of the interesting IP anomalies detected during the TDIP survey carried during this year. The location of the 600m by 600m-large fixed loops is indicated in the TDIP plane maps of Fig. II-5-18. The loop was centered on the lowest resistivity anomaly detected between 2600E to 3000E and 1500N to 1700N.

(2) Results

Loop 2

The data was processed by subtraction from a three-layer earth (host rock) response. The host rock response was calculated from the following model:

- An upper layer of 350 Ωm, 170m thickness
- An intermediate layer of 1600 Ωm, 70m thickness
- A basement layer of 200 Ωm.

Figs. II-6-5(1) and II-6-5(2) show the contour maps of the TEM responses obtained in each of the 20 channels.

At low and intermediate channels (1 to 12), a broad high TEM response centered on the station 2800E, 1500N was detected in the central-south part of the loop. To confirm the high response, a hole was drilled around the center of this TEM anomaly; however, the results were not entirely satisfactory. This anomaly changes abruptly after channel 14, indicating that conductivity is seen only at shallow and intermediate levels.

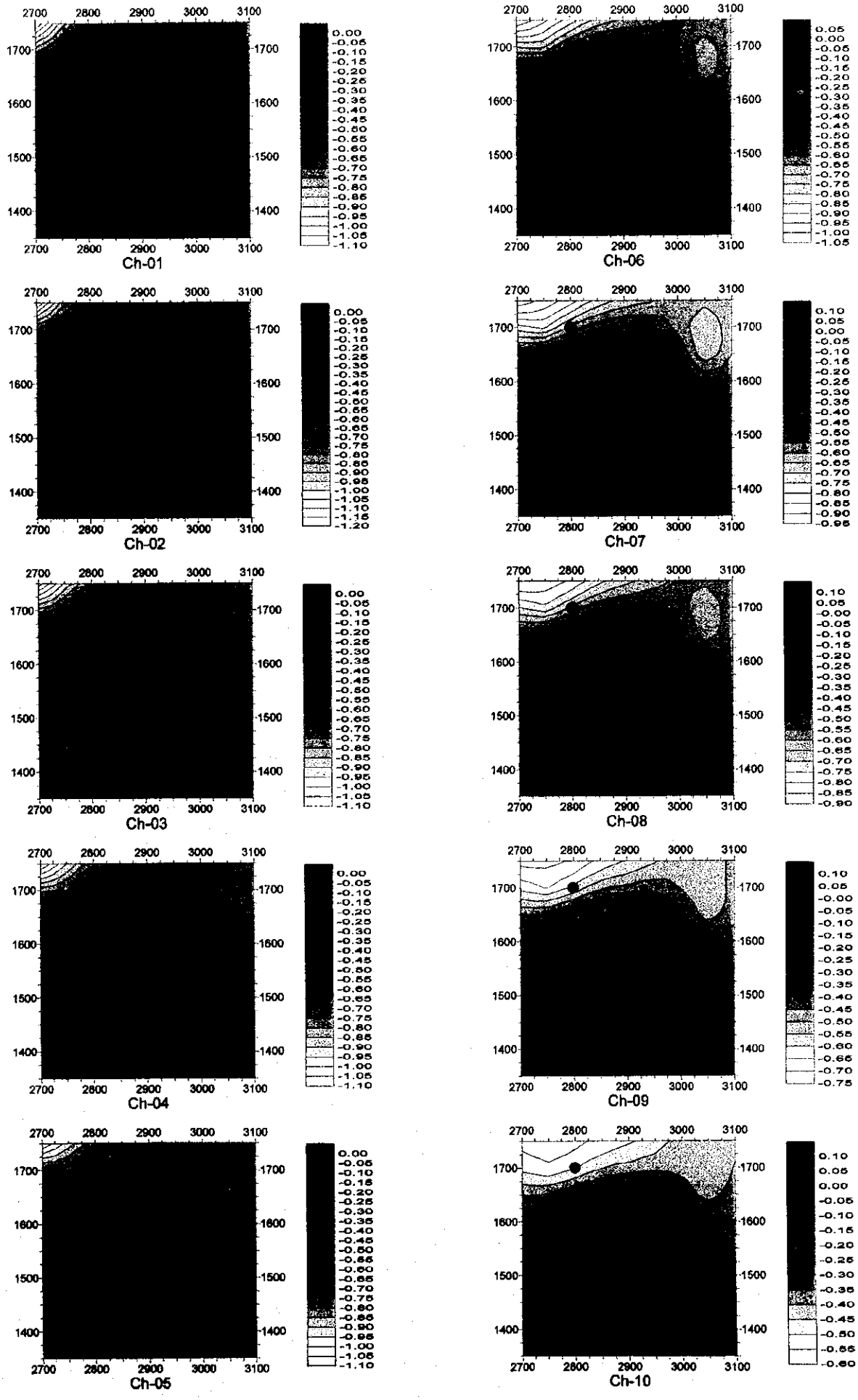

Fig. Ⅱ-6-5(1) TEM response maps of Loop2 (Ch1-Ch10)

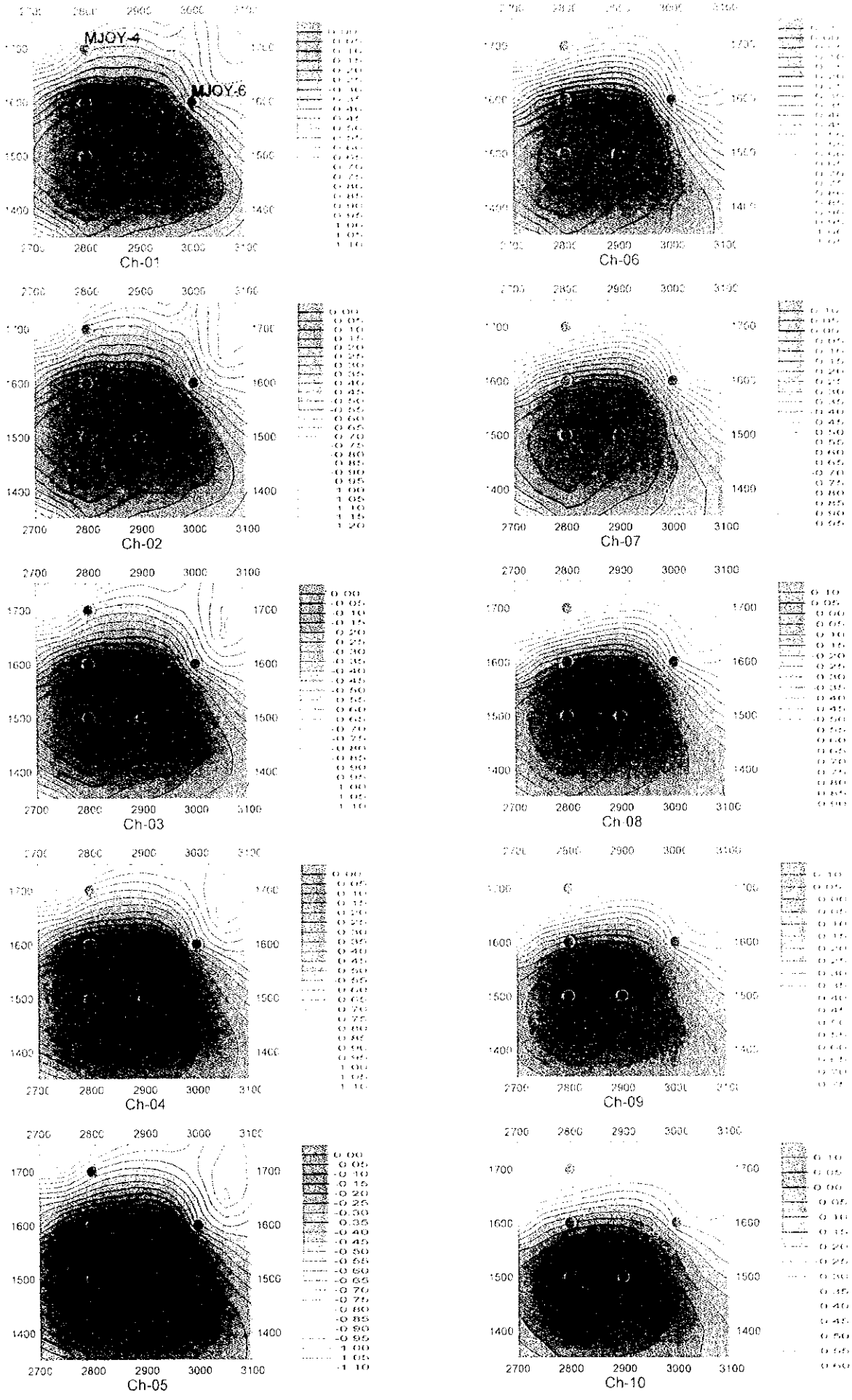

Fig. II-6-5(1) TEM response maps of Loop2 (Ch1-Ch10)

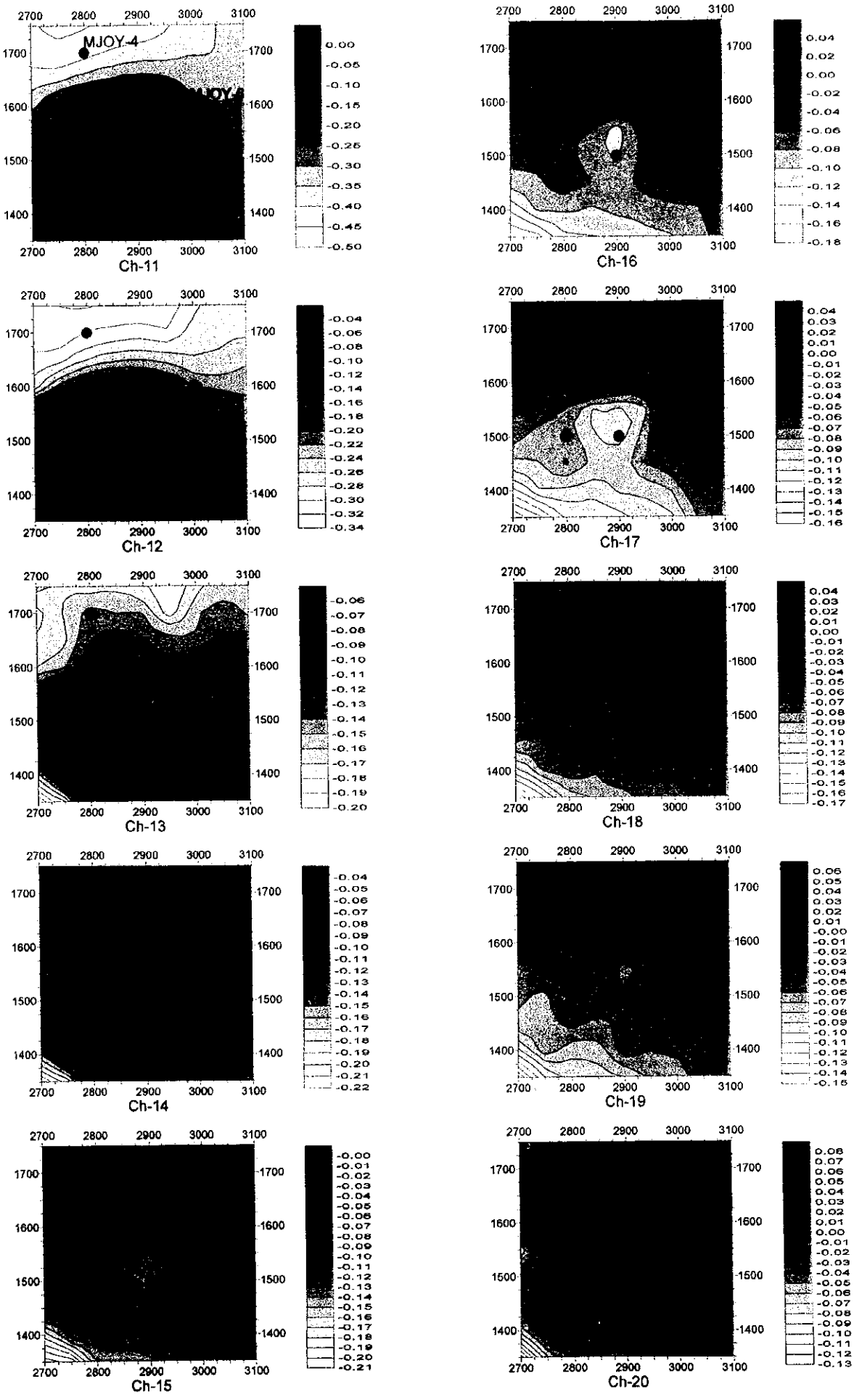

Fig. II-6-5(2) TEM response maps of Loop2 (Ch11-Ch20)

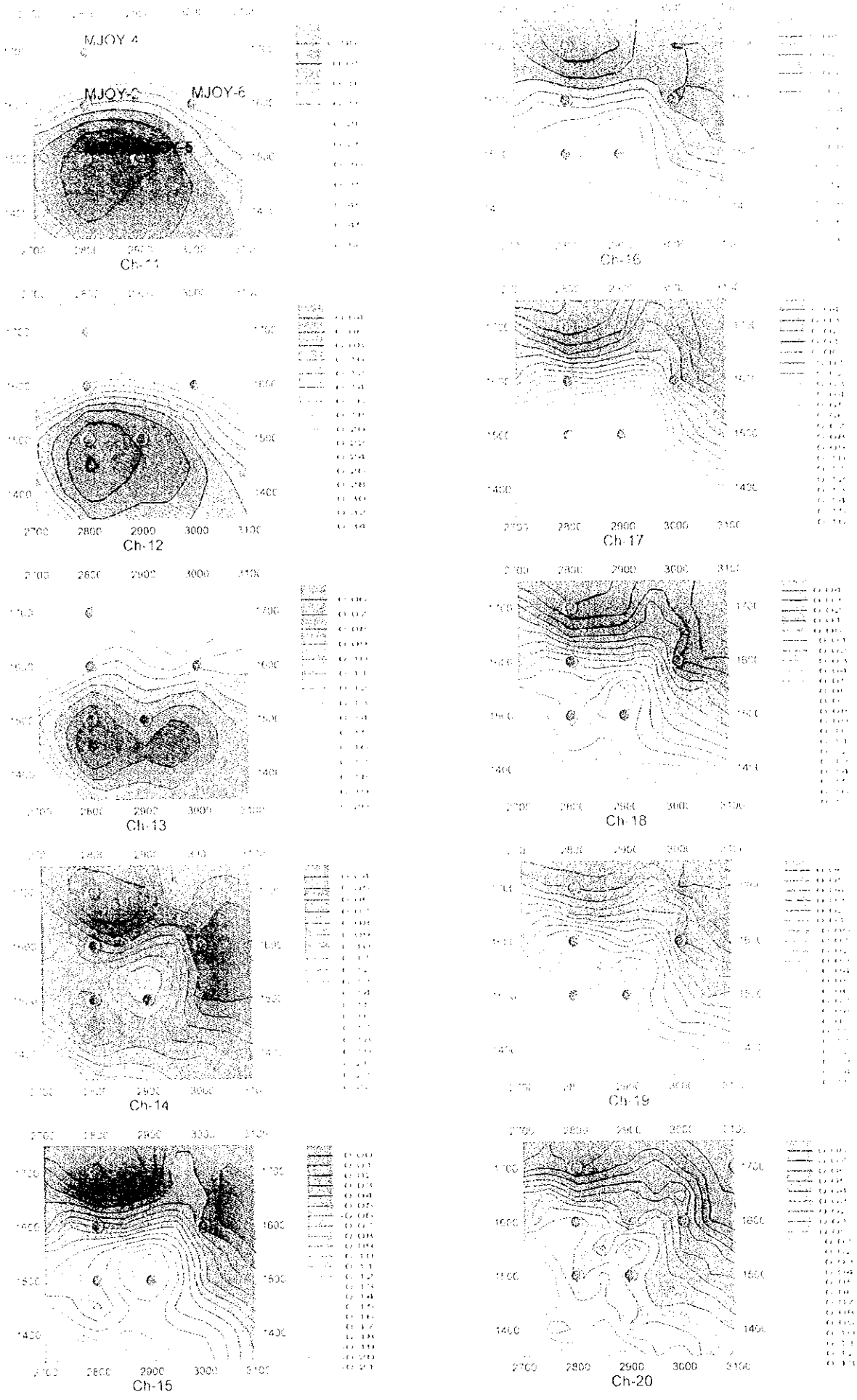

Fig. II-6-5(2) HEM response maps of Loop2 (Ch11-Ch20)

To confirm further this anomaly and the interesting IP results, 2 more holes were drilled within this anomaly and 2 more at the outskirt of the TEM anomaly but within the high chargeability zone. The locations of these drillings are also indicated in the above-mentioned figures.

6-5-3 Hayl as Safil anomaly

(1) Loops location

As indicated by the TDIP geophysical results shown in the plane maps of Figs. II-2-23, several interesting anomalies were detected within places where the ore bodies of Bishara, Safil and Jadded are located. Especially interesting low resistivity results accompanied by chargeability were detected to the south of 1800N. To further study these results, 5 loops were set up on these anomalies as indicated on Figs. II-2-23.

(2) Results

The data collected from the 5 loops was processed by subtraction from a two-layer earth (host rock) response. The host rock response was calculated from the following model:

- An upper layer of 80Ωm, 200m thickness
- A basement layer of 1500 Ωm.

Loop 3 (Fig. II-6-6)

Located around the main gossan, a high TEM response distribution is detected along the SW corner of the loop and passing through the center. Two high TEM responses were detected along this trending, i.e., one around the station 3800W, 1500N, and another one around the station 3700W, 1700N, both seen at the intermediate channels from 5 to 15. Even though there seems to be a good correspondence between these results and the resistivity distributions calculated by the 2D modeling, the TEM response is not as remarkable as the low resistivity detected by the TDIP survey.

Loop 4 (Fig. II-6-7)

Placed to the east side of Loop 3. In correspondence with the 2D calculation of the TDIP survey, there is no remarkable anomaly detected, except for the SW corner of the loop where a continuation of the remarkable IP anomaly detected in the previous loop is seen here. High TEM response is seen only at deep levels but the continuous trending dose not give indication of a promising anomaly.

Loop 5 (Fig. II-6-8)

Located to the south side of Loop 3. The same low resistivity NW-SE trending seen in the south-central side of the 2D calculations of the TDIP results is seen as high TEM responses, however no clear anomaly is detected that can suggest the presence of massive sulphide.

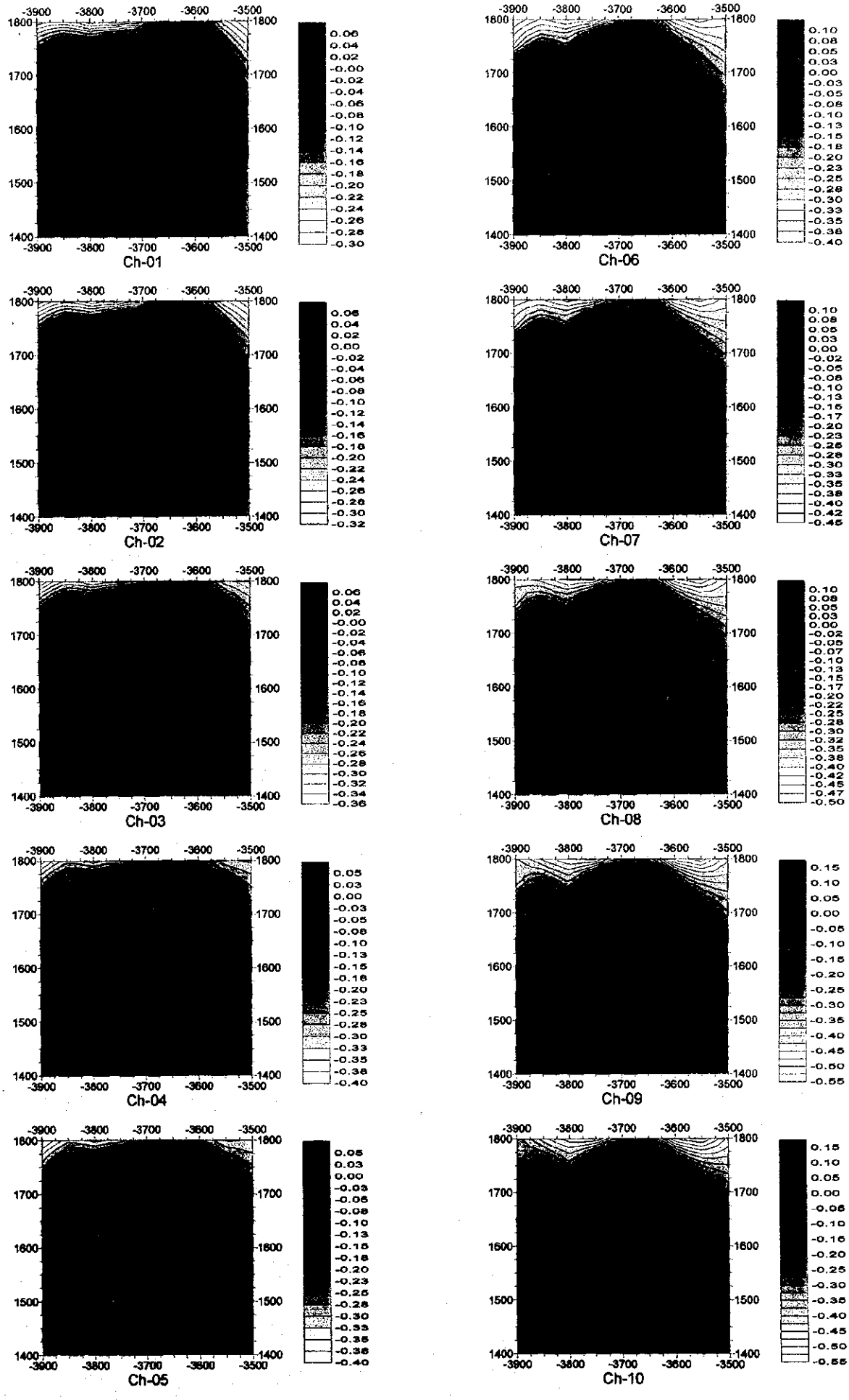

Fig. II-6-6(1) TEM response maps of Loop3 (Ch1-Ch10)

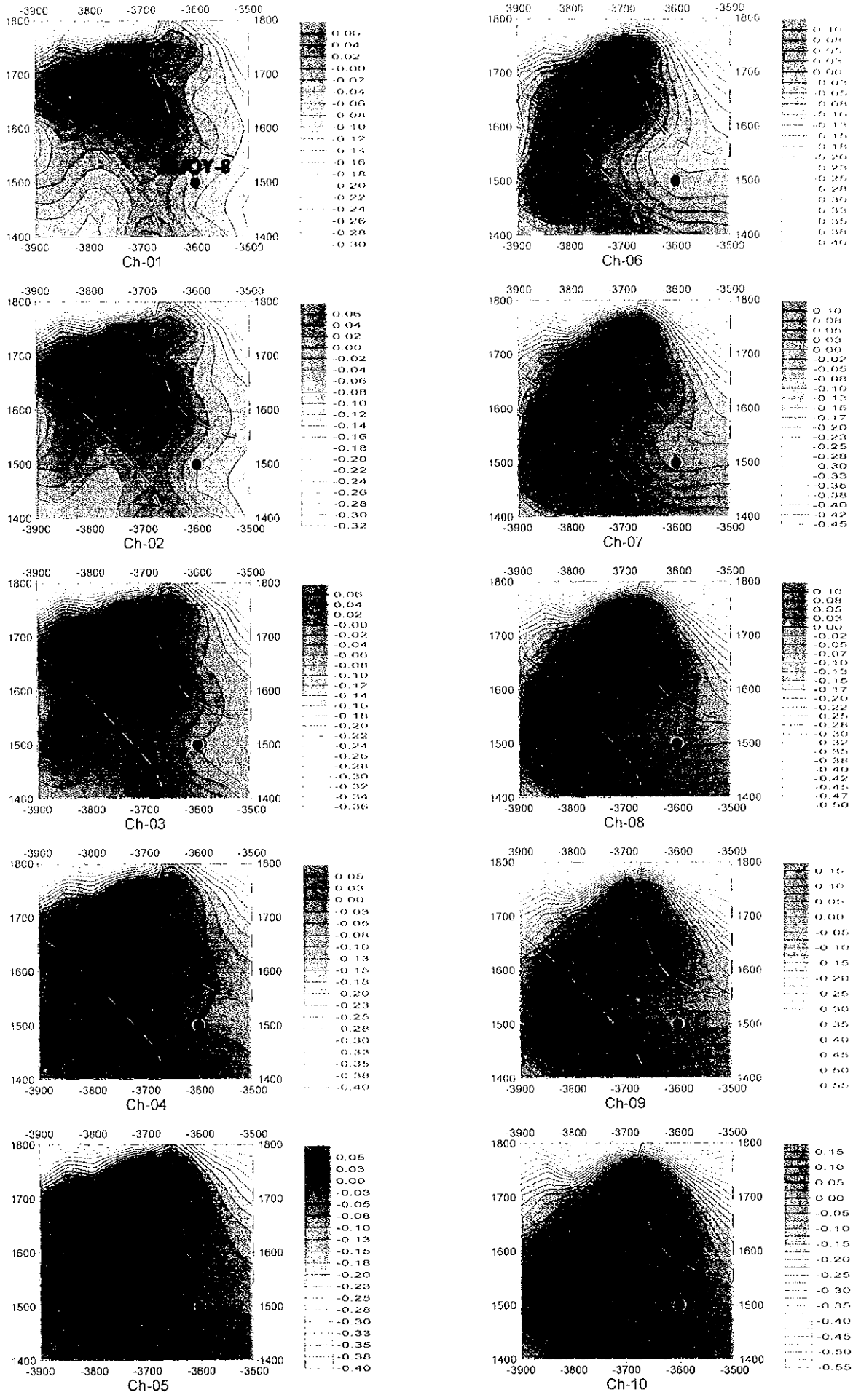

Fig. II-6-6(1) TEM response maps of Loop3 (Ch1-Ch10)

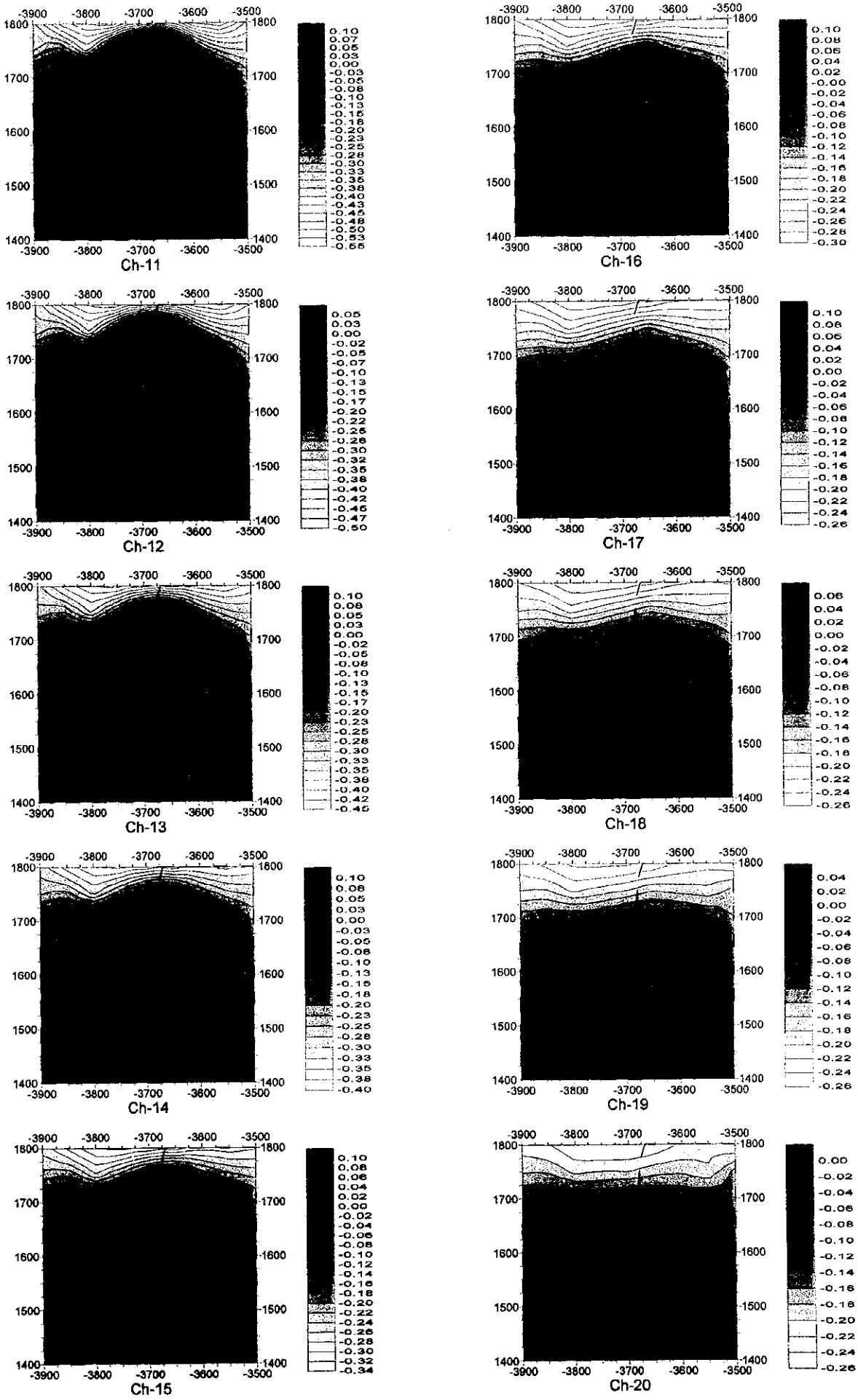

Fig. II -6-6(2) TEM response maps of Loop3 (Ch11-Ch20)

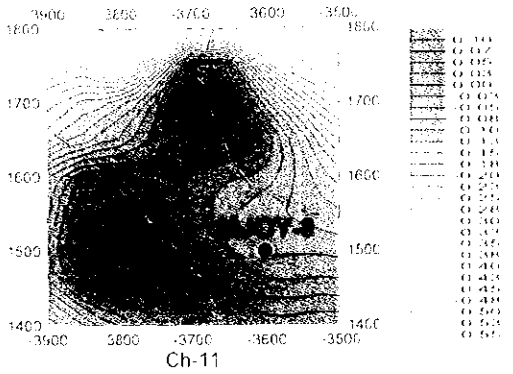

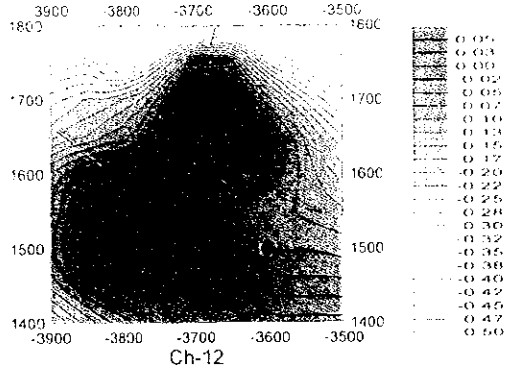

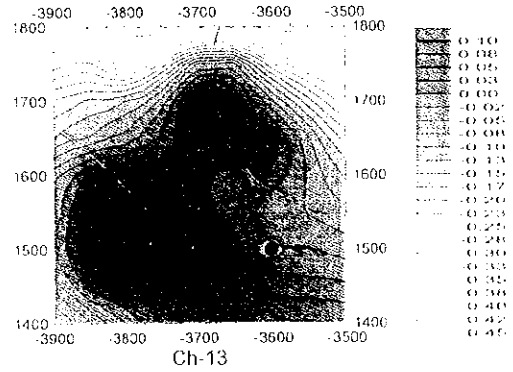

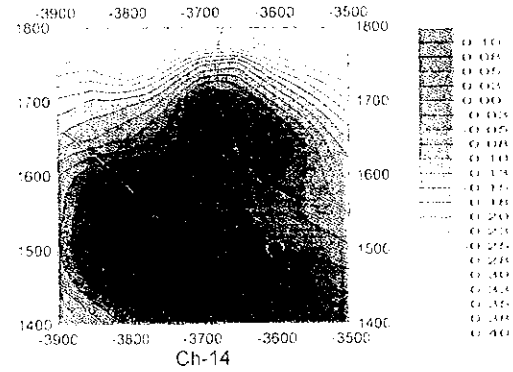

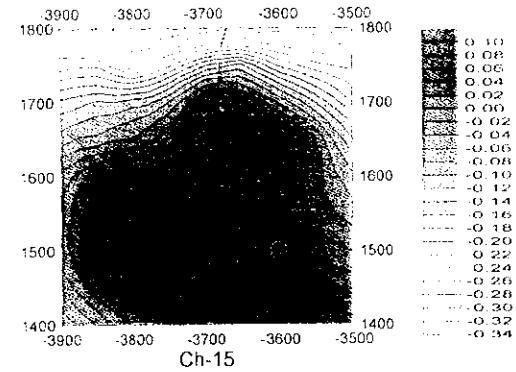

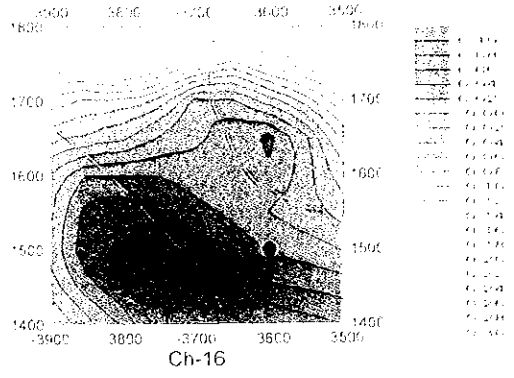

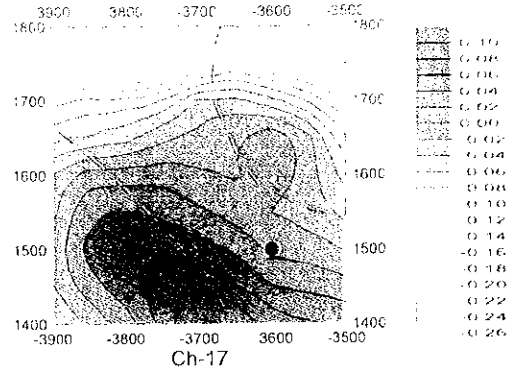

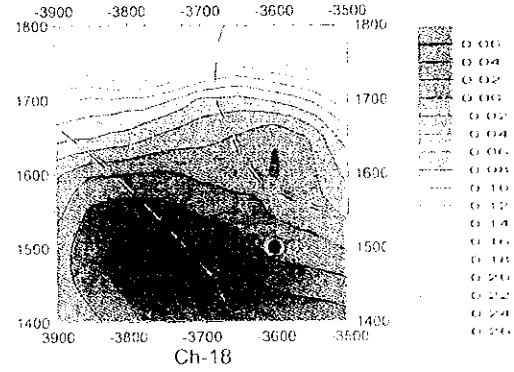

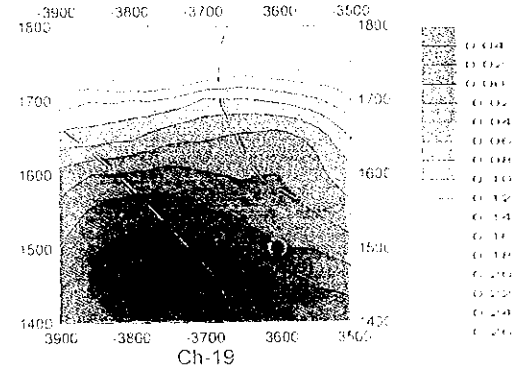

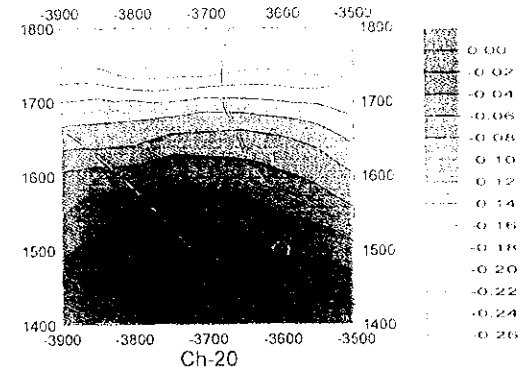

Fig. II-6-6(2) TEM response maps of Loop3 (Ch11-Ch20)

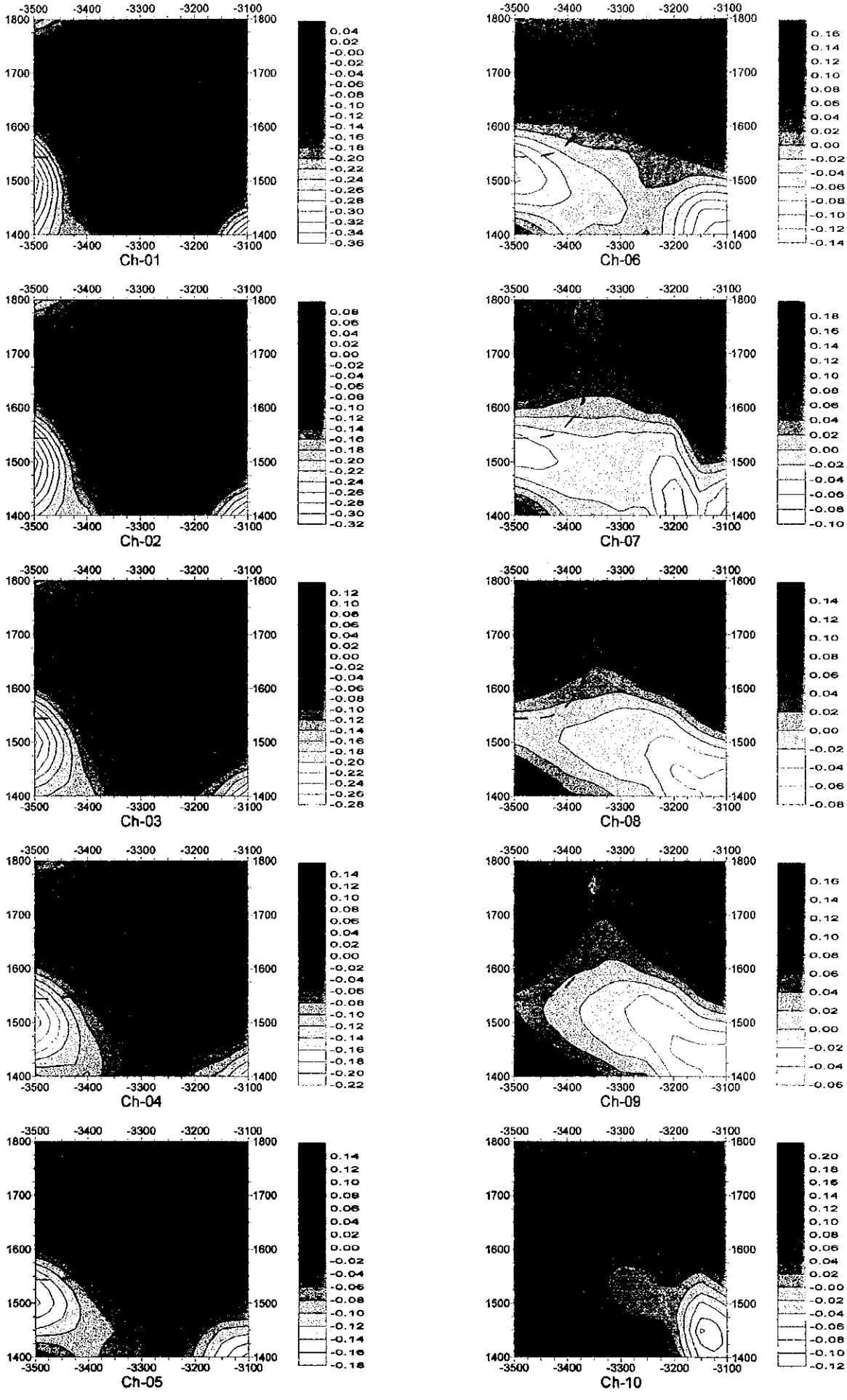

Fig. II-6-7(1) TEM response maps of Loop4 (Ch1-Ch10)

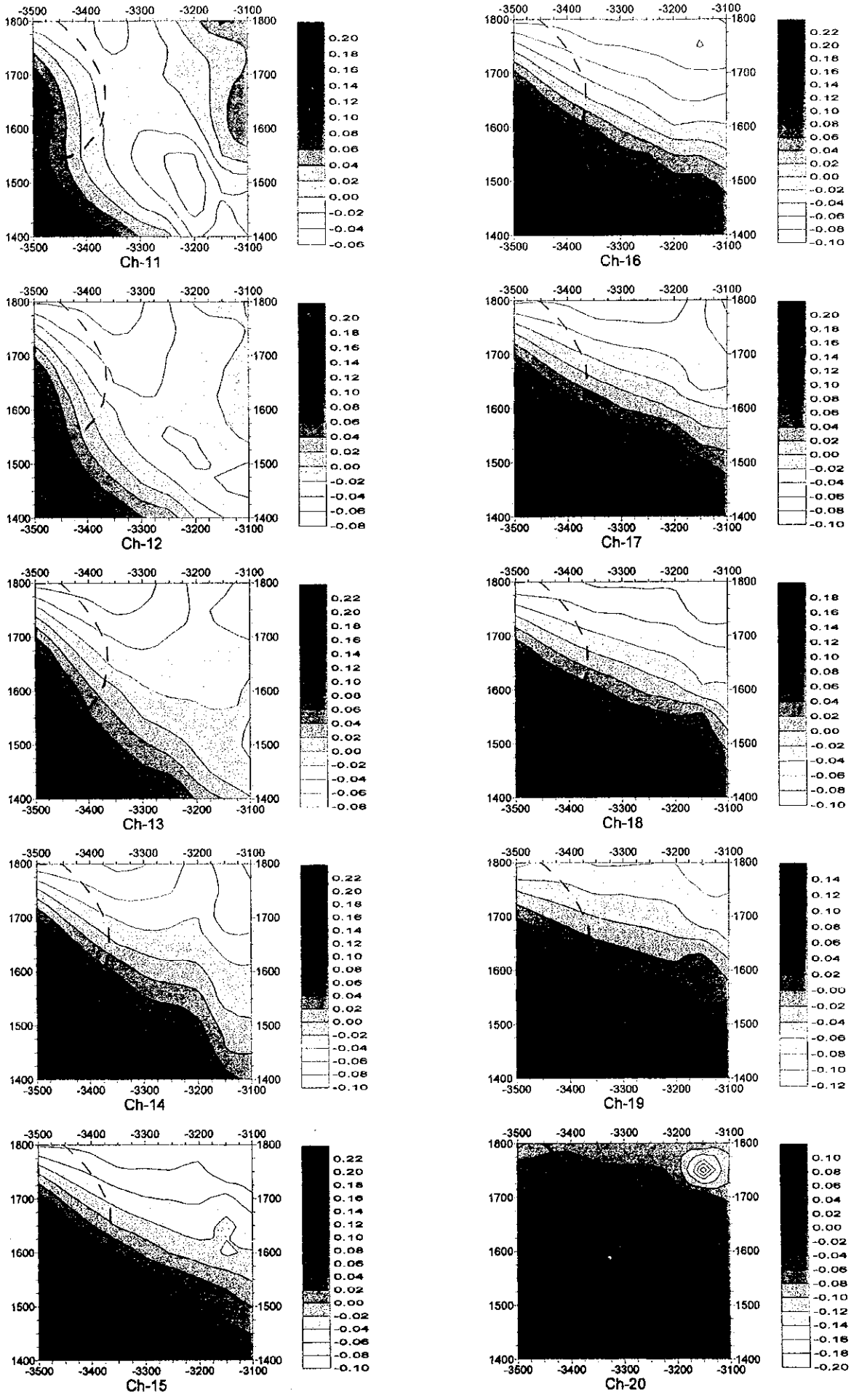

Fig. II-6-7(2) TEM response maps of Loop4 (Ch11-Ch20)

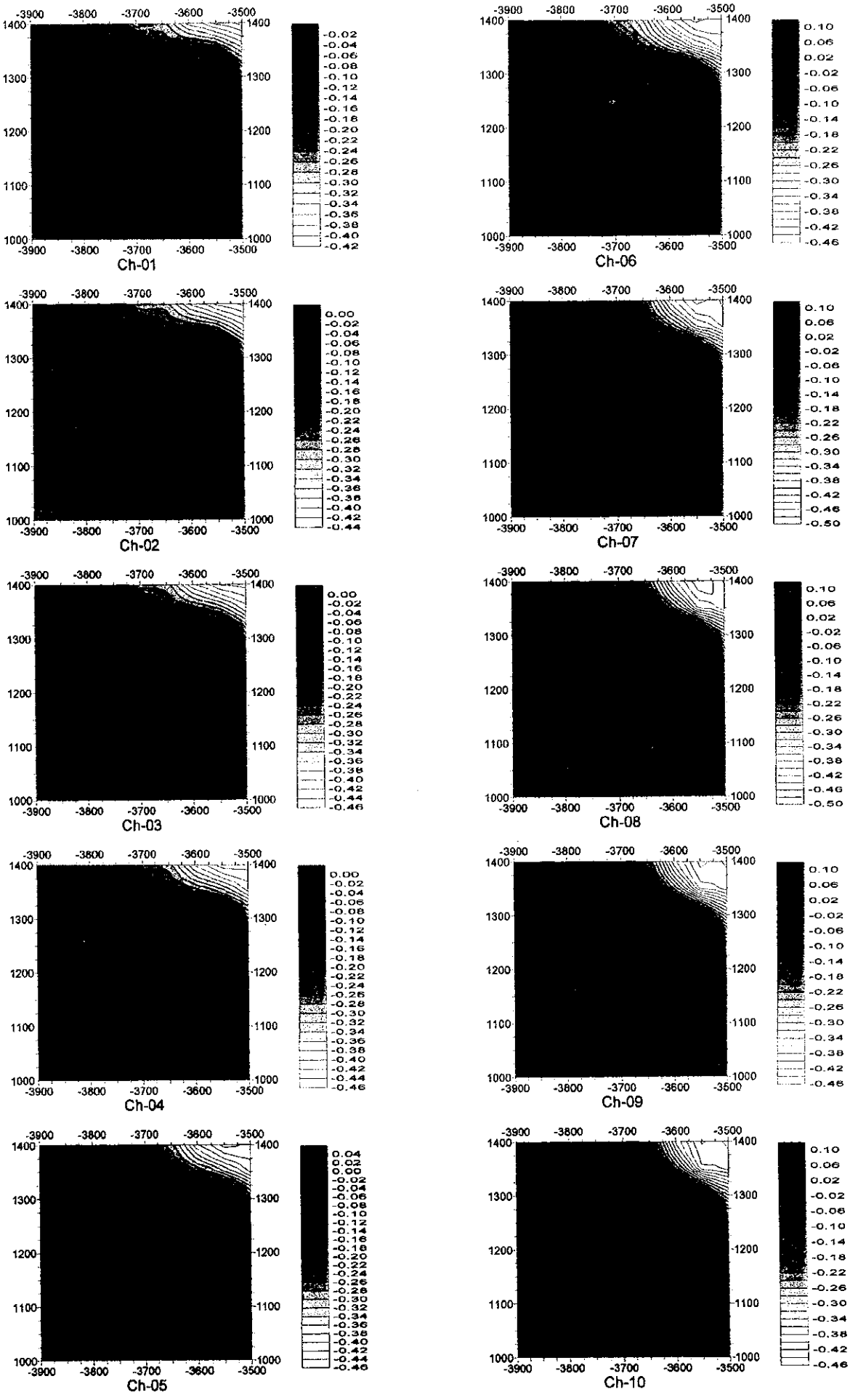

Fig. Ⅱ-6-8(1) TEM response maps of Loop5 (Ch1-Ch10)

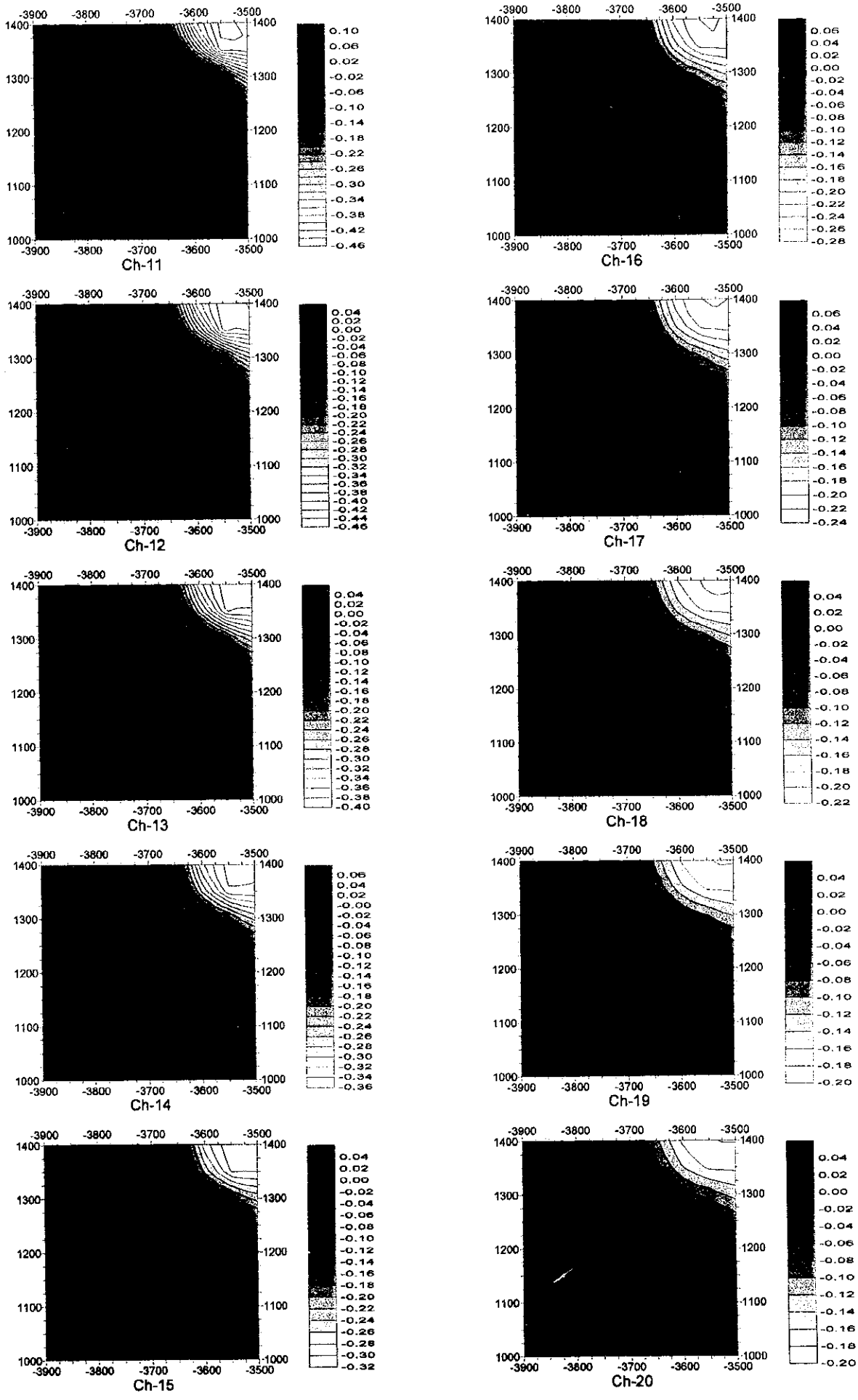

Fig. II-6-8(2) TEM response maps of Loop5 (Ch11-Ch20)